

Lanthanide Directed Self-Assembly of Highly Luminescent Supramolecular “Peptide” Bundles from α -Amino Acid Functionalized 2,6-Bis(1,2,3-triazol-4-yl)pyridine (btp) Ligands

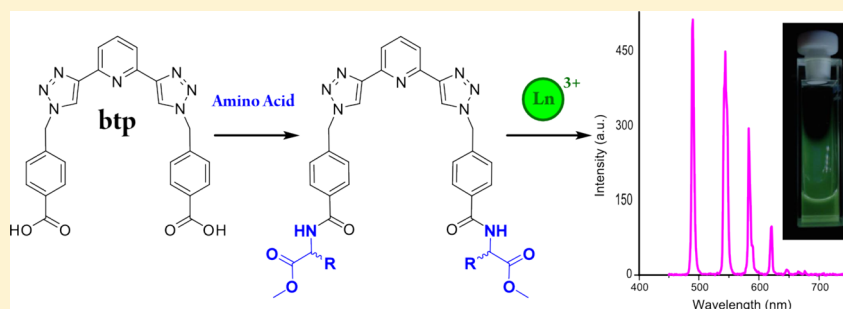
Joseph P. Byrne,[†] Jonathan A. Kitchen,^{†,‡} John E. O’Brien,[†] Robert D. Peacock,[§] and Thorfinnur Gunnlaugsson^{*,†}

[†]School of Chemistry and Trinity Biomedical Sciences Institute, Trinity College Dublin, University of Dublin, Pearse Street, Dublin 2, Ireland

[‡]Chemistry, Faculty of Natural & Environmental Sciences, University of Southampton, Highfield, Southampton SO17 1BJ, U.K.

[§]School of Chemistry, University of Glasgow, Glasgow, G12 8QQ, Scotland, U.K.

S Supporting Information



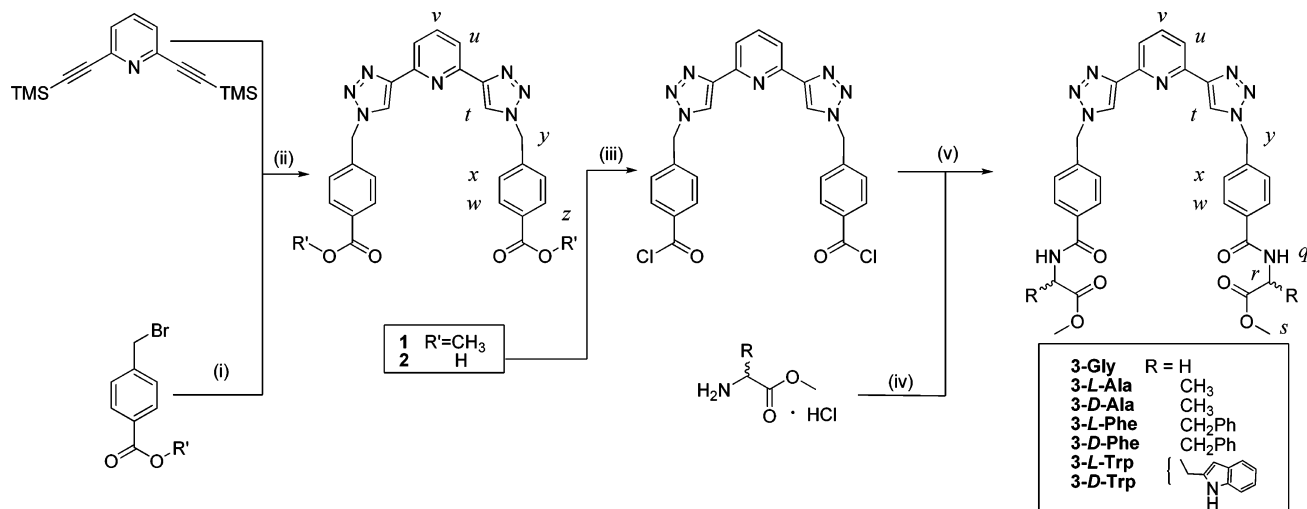
ABSTRACT: Ligands containing the [2,6-bis(1,2,3-triazol-4-yl)pyridine] (**btp**) motif have recently shown promise in coordination chemistry. The motif is synthesized via the Cu(I)-catalyzed “click” reaction and can be conveniently functionalized when compared to other terdentate chelating motifs. Ligand **1** was synthesized and shown to sensitize Eu(III) and Tb(III) excited states effectively. The use of these ions to synthesize self-assembly structures in solution was investigated by carrying out both ¹H NMR and photophysical titrations. The latter were used to determine high binding constants from changes in the absorption, ligand emission (fluorescence), and lanthanide-centered emission. A small library of amino acid derivatives of **1**, ligands **3**, were prepared upon coupling reactions with Gly, Ala, Phe, and Trp methyl esters, with a view to introducing biologically relevant and chiral moieties into such ligands. All of these derivatives were shown to form stable, emissive Ln(III) self-assemblies, emitting in the millisecond time range, which were studied by means of probing their photophysical properties in organic solutions using lanthanide ion titrations. All the Tb(III) complexes, with the exception of Trp based derivatives, gave rise to highly luminescent and bright complexes, with quantum yields of Tb(III) emission of 46–70% in CH₃CN solution. In contrast, the Eu(III) complexes gave rise to more modest quantum yields of 0.3–3%, reflecting better energy match for the Tb(III) complexes, and hence, more efficient sensitization, as demonstrated by using low temperature measurements to determine the triplet state of **1**.

INTRODUCTION

The 2,6-bis(1,2,3-triazol-4-yl)pyridine (**btp**) motif has attracted significant attention in recent years^{1,2} (e.g., from researchers such as Crowley,^{2,3} Flood,^{4–6} Hecht,^{7–10} and Schubert^{11–15}) as a class of pyridine-centered terdentate ligands with applications in supramolecular and coordination chemistry. The **btp** ligands possess similar bond lengths and angles to the widely used 2,2';6',2''-terpyridine (**terpy**) binding motif, and as such are highly desirable alternatives to **terpy** in coordination chemistry;¹⁶ however, their exploitation has been somewhat limited to date. We have recently reviewed the relatively small amount of literature surrounding the use of the **btp** motif in supramolecular and coordination chemistry, and in the process, have highlighted the potential that such a modular and

synthetically flexible motif has in modern supramolecular chemistry.¹⁷ Herein, we describe our recent efforts into developing self-assembly structures from amino acid derived **btp** ligands, by employing lanthanide directed synthesis. A key attractive feature of the **btp** ligands is that they can be prepared in a facile one-pot synthesis using the Cu(I)-catalyzed alkyne–azide “click” (CuAAC) reaction from a wide range of azide substrates, allowing for convenient derivatization and variety in such ligands.^{2,10,18,19} The coordination chemistry of ligands containing this motif has been studied with many metal ions including Ni(II),²⁰ Cu(I),²¹ Cu(II),^{2,22} Zn(II),²³ Ag(I),²

Received: October 1, 2014

Scheme 1. Synthesis of Ligands 1–3^a

^a(i) NaN₃, rt, 1 h, DMF/H₂O; (ii) CuSO₄·5H₂O, sodium ascorbate, K₂CO₃, DMF/H₂O, rt, 18 h; (iii) SOCl₂, Δ, 18 h; (iv) Et₃N, rt, 1 h; (v) CH₂Cl₂, rt, 18 h.

Ir(III),²⁰ Pt(II),^{14,24} Pd(II),²⁵ Pb(II),²⁶ Fe(II),^{1,10,23} and Ru(II).^{1,11–16,18,23,27–29} The most studied of these, by far, is Ru(II). Hecht and co-workers have prepared a range of mono- and dileptic Ru(II)–**btp** complexes and tuned their electrochemical properties upon variation of the ligand.²³ Schubert and co-workers compared such systems' photophysical behavior with analogous **terpy**-based systems and also reported mixed heteroleptic **terpy**–**btp** complexes with intermediate properties.^{11,12,27} We recently published the synthesis and characterization of two **btp** ligands, **1** and **2**, and studied their coordination chemistry with a number of d-block metals (namely, Ru(II), Ir(III), Ni(II), and Pt(II)), as well as their photophysical properties and the electrochemical properties of the Ru(II) complexes.²⁰ We also demonstrated that these ligands can give rise to the formation of metallogels with some of these ions. There is, however, a surprising paucity in the literature of examples of **btp** systems coordinating the f-block lanthanide(III) (Ln(III)) ions. Ln(III) have been exploited for the formation of elegant self-assembly systems such as polymetallic helicates.³⁰ They possess unique photophysical and magnetic properties, which make their study desirable for optoelectronic and bioimaging applications.^{31–33} Hence, the need to explore the **btp** motif within lanthanide chemistry prompted us to develop the work presented here, focusing on the use of Ln(III) ions to direct, through their high coordination requirements, the formation of novel functional and luminescent supramolecular self-assembly structures.

In the past, we have shown how Ln(III) is capable of forming self-assemblies, such as bundles,³⁴ helicates,³⁵ half-helicates,³⁶ and interlocked systems such as a [3]catenane,³⁷ with dipicolinic acid (**dpa**) derivatives, as well as luminescent Langmuir–Blodgett films^{38,39} and supramolecular gels based on the **terpy** motif.⁴⁰ Indeed, many researchers have shown how other pyridine-centered terdentate ligands, particularly motifs which contain heterocyclic rings, have been widely exploited to form luminescent Ln(III)-directed structures, including the benzimidazole-based systems studied at length by Piguet, Bünzli, and co-workers,^{41–43} the **pybox** ligands (2,6-bis-(oxazoline)pyridine) employed by the group of de Bettencourt-Dias,^{44–46} and the highly emissive Ln(III) complexes of

pyridine-bis(tetrazolate) systems developed by Mazzanti and co-workers.^{47,48} We herein present an investigation of the self-assembly behavior of **btp** ligands **1**, and **3** with Eu(III) and Tb(III) ions, the outcome of which we describe as lanthanide directed synthesis of “peptide bundles”. Flood et al. displayed that **btp** compounds can form stable coordination compounds with Eu(III), sensitizing characteristic line-like emission from the metal center via the “antenna effect”,¹ while Hecht and co-workers also reported Eu(III) complexes.¹⁰ “Back-to-back” ditopic **btp** ligands have also been used to sensitize Ln(III) luminescence.⁴⁹ Brunet and co-workers described covalently attaching **btp**-containing organic phosphonates to the surface of the γ -zirconium phosphate by topotactic exchange to produce a solid host that could efficiently sensitize the emission of Ln(III) ions.^{19,50} O'Reilly and co-workers used Eu(III) coordinated by **btp** ligands containing RAFT polymerization agents to template “star-branched” polymeric structures.¹⁸ We herein present an investigation of the self-assembly behavior of **btp** ligand **1** with Eu(III) and Tb(III) ions. More recently, a number of Ln(III) complexes of bis(benzyl)-**btp** have been evaluated as chemically stable bioimaging agents, suggesting the potential utility of such compounds for biological applications.⁵¹ With the aim of introducing biorelevant moieties into these compounds, we prepared derivatives of **1** with appended amino acid methyl ester residues, ligands **3**. Amino acids are small, convenient, and mostly chiral residues, which are ubiquitous in nature, acting as the building blocks for peptides and proteins. Their incorporation into **btp** ligands provides a facile route toward a range of derivatives **3**, which were all chiral, apart from **3-Gly**, which contains the optically inactive Gly residue. The ligands were prepared through straightforward amide coupling reactions. The synthesis and characterization of seven such ligands and their Eu(III) and Tb(III) complexes are reported as well as their self-assembly behavior in CH₃CN solution, allowing the determination of global stability constants for various stoichiometric species. Such self-assembly structures can be considered as ternary structural building units with the potential to function as a foundation for tertiary peptide structural mimics; we have recently demonstrated that peptide conjugates (of up to 20-mers) can form highly ordered

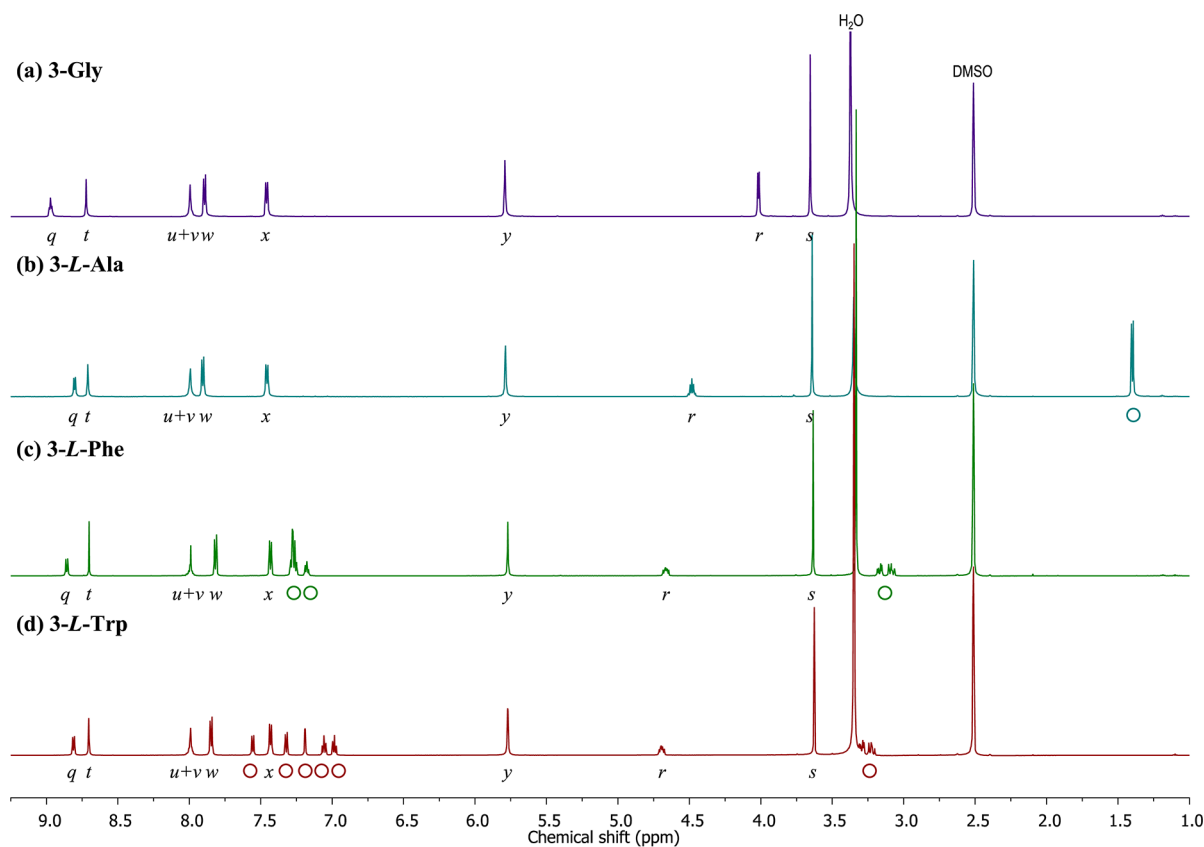


Figure 1. ^1H NMR spectra (600 MHz, $\text{DMSO-}d_6$) of ligands (a) 3-Gly, (b) 3-L-Ala, (c) 3-L-Phe and (d) 3-L-Trp (resonance at 10.5 ppm from indolyl NH not shown). Resonances are labeled as follows: *q* (amide NH), *r* (α -protons in amino acid residue), *s* ($-\text{OCH}_3$), *t* (triazolyl CH), *u* (3- and 5-pyridyl CH), *v* (4-pyridyl CH), *w* and *x* (phenyl CH), *y* (CH_2), \circ (peaks particular to amino acid side-chain). (Spectra of 3-D-Ala, 3-D-Phe, and 3-D-Trp were identical to their enantiomers and are shown in Supporting Information.)

folded structures through the use of lanthanide directed synthesis, where the changes in the lanthanide centered emission were monitored upon folding.⁵²

RESULTS AND DISCUSSION

Ligand Synthesis, Characterization, and Photophysical Properties. Ligands **1** and **2** were prepared using a one-pot deprotection/“click” CuAAC reaction in high purity and moderate yields of 53% and 63%, respectively, as previously reported.²⁰ The carboxylic acid ligand **2** proved to have poor solubility in many organic solvents. Ligand **1**, however, was readily soluble in a range of solvents. Methyl ester-protected amino acids were coupled with both carboxylic acid groups of ligand **2** in order to produce a small library of bis-substituted **btp** ligands, **3** (see table in Scheme 1). This was achieved as shown in Scheme 1 by first converting **2** into its acid chloride derivative with thionyl chloride. The methyl ester-protected amino acids (as HCl salts), Gly, Ala, Phe, and Trp (the latter of which has been employed in the literature as a naturally occurring antenna for Tb(III) emission^{53,54}) were first stirred with Et_3N in CH_2Cl_2 for an hour, before being added to the acid chloride and stirred at room temperature. Both the *L*- and the *D*-enantiomers of the chiral amino acids Ala, Phe, and Trp were used. Solvent was removed and the product was triturated with cold CH_3OH , furnishing the amide products in moderate yields (47–61%) and high purity upon filtration (as confirmed by elemental analysis).

The simplicity of the ^1H NMR spectra (600 MHz, $\text{DMSO-}d_6$) of **3** confirmed the formation of ligands possessing C_2

symmetry, only differing significantly from the previously reported spectra of **1** and **2**²⁰ in the presence of resonances arising from the amino acid moieties, with the spectra of enantiomeric pairs being identical (cf. Supporting Information); hence only the ligands containing two *L*-amino acid residues as “arms” will be discussed here. The ^1H NMR spectrum (600 MHz, $\text{DMSO-}d_6$) of 3-Gly, shown in Figure 1a, displayed a resonance relating to the methyl ester protecting group at 3.65 ppm (labeled *s*), a doublet arising from the Gly CH_2 at 4.02 ppm (*r*) and a signal at 5.79 ppm from the methylene linker between the triazole and phenyl rings (*y*). The aromatic region consisted of a pair of phenyl doublets at 7.46 and 7.89 ppm, two pyridyl resonances, overlapping as a multiplet from 7.93–8.05 ppm (*u* and *v*), a triazolyl resonance at 8.72 ppm (*t*), and a triplet resonating at 8.97 ppm assigned to the amide NH protons (*q*). All NH proton resonances were assigned by NH COSY, see Supporting Information. ESI MS analysis confirmed the identity of the desired product. As expected, the ^1H NMR spectrum (600 MHz, $\text{DMSO-}d_6$) of 3-L-Ala was very similar to that of the Gly derivative above, differing only in the presence of the chiral side-chain, resonating at 1.40 ppm as a doublet (marked in Figure 1b with a \circ) and a resonance centered at 4.48 ppm arising from the adjacent chiral CH (*r*) of the Ala residue. The NH resonance was also shifted to lower frequency, appearing as a doublet at 8.81 ppm. Similarly, the 3-L-Phe ^1H NMR spectrum (600 MHz, $\text{DMSO-}d_6$, Figure 1c) closely resembled the Ala derivative described above, the benzyl CH_2 protons appearing as multiplets between 3.05–3.19 ppm and the α -protons at 4.66

ppm with further resonances occurring at 7.15–7.20 and 7.25–7.30 ppm, for the aryl protons. Again, the amide NH resonance (*q*) appeared at a different chemical shift of 8.86 ppm.

The ^1H NMR spectrum (600 MHz, $\text{DMSO-}d_6$) of **3-L-Trp** was the most complicated of the ligands described herein, as is evident from Figure 1d, with aliphatic resonances similar to those seen for **3-L-Phe**; the indole peaks appeared as a pair of triplets at 6.98 and 7.06 ppm and three doublets at 7.19, 7.32, and 7.55 ppm. These resonances were well resolved from the two phenyl CH doublets at 7.43 and 7.84 ppm (labeled *x* and *w*, respectively), the pyridyl multiplet at 7.96–8.03 ppm and the triazolyl resonance at 8.70 ppm (*t*). **3-L-Trp** showed two NH resonances. The amide signal appeared as a doublet at 8.81 ppm, while the indole NH resonated at a higher frequency of 10.80 ppm (see Supporting Information). ESI MS analysis confirmed the identity of all the aforementioned ligands.

General Photophysical Properties of 3. Ligands **1**, **3-Gly**, **3-Ala**, and **3-Phe** showed broadly similar UV–vis absorption profiles when recorded in CH_3CN solution, Figure 2, with distinct bands centered at 300 nm, tentatively assigned to $n \rightarrow \pi^*$ transitions from the **btp** core, and 235 nm, assigned to $\pi \rightarrow \pi^*$ transitions from the various aromatic rings in the structures. For **3-Phe**, the lower wavelength band was broader and only slightly shifted by a few nanometres relative to the parent ligand **1** ($\lambda_{\text{max}} = 237$ nm). **3-Trp** shows a broader

absorption profile with a maximum centered at 223 nm, a shoulder around 235 nm, and a sharp peak at $\lambda_{\text{max}} = 290$ nm overlapping with a broader band resembling the 300 nm-band in all of the other ligands. This is consistent with the absorption profile of Trp-containing ligands reported by us previously.⁵⁵ Upon excitation into either band, **1** displayed a broad fluorescence band centered at 335 nm. Ligands **3** all showed a similar emission band. Excitation spectra of this emission across the range of ligands were practically identical and matched the general structure of the absorption profiles, the exception being **3-Trp**, where the excitation spectrum resembled just those bands associated with the **btp** “core” and not those assigned to the Trp moieties (*viz.* the bands at 223 and 290 nm). This suggested that fluorescence arises largely from the **btp** moiety of these ligands. CD spectra of ligands **3** were weak and poorly resolved, but did show subtle differences between the enantiomers.

Preparation and Photophysical Studies of Ln(III) Complexes. Having synthesized the above ligands **1** and **3**, both Eu(III) and Tb(III) complexes were prepared from these ligands. This was achieved using microwave irradiation of **1** or **3** in the presence of 0.35 equiv of Eu(III) or Tb(III) triflate salt in CH_3OH solution at 70 °C for 20 min. The complexes were recovered as solids upon diffusion of Et_2O into the CH_3OH solution, with successful complexation being confirmed by MALDI+ mass spectrometry, Table 1, where the characteristic isotopic distribution patterns of the measured peaks matched the calculated spectra (see Supporting Information). Evidence was also seen in the MALDI+ spectra of fragmentation into the 1:2 and, in some cases, 1:1 stoichiometries. These peaks are listed with the experimental details. Unfortunately, we were unable to obtain crystals of these systems of sufficient quality for crystal structural analysis, and hence, their structural nature was probed by using solution state analysis only, such as UV–vis absorption, emission and NMR analysis.

Compared to the UV–vis absorption spectra of the relevant ligands, upon complexation with either Eu(III) or Tb(III), the ligand band centered at 300 nm (assigned to the **btp** center) was red-shifted to ~ 313 nm, indicating the successful formation of the complexes. IR spectra were also altered upon formation of the complexes.

All the complexes showed characteristic Ln(III)-centered emission spectra upon excitation of the pyridine moiety, confirming the ability of the **btp** ligands to sensitize the Ln(III) excited states in these complexes successfully (see Supporting Information), while, in contrast, ligand fluorescence was quenched. For Eu(III) complexes, characteristic line-like emission bands were observed at $\lambda = 579, 593, 617, 650,$ and 694 nm, assigned to the $^5\text{D}_0 \rightarrow ^7\text{F}_j$ transitions ($J = 0-4$), as demonstrated in Figure 3a, for $[\text{Eu}(\text{3-L-Phe})_3](\text{CF}_3\text{SO}_3)_3$. In the case of the Tb(III) complexes, Tb(III)-centered emission bands were observed at 490, 545, 585, and 621 nm, assigned to the $^5\text{D}_4 \rightarrow ^7\text{F}_j$ transitions ($J = 6-3$) of Tb(III), as well as weaker bands arising from the transitions to the $J = 2-0$ states, Figure 3b. The sensitization process was further confirmed by recording the excitation spectra of the various Ln(III) complexes, which were seen to structurally match the absorption spectra. Moreover, the complexes were clearly luminescent to the naked eye, even at low concentrations, upon irradiation with a hand-held UV lamp, as is demonstrated by the photographs of CH_3CN solutions of Ln(III) complexes shown as insets in Figure 3.

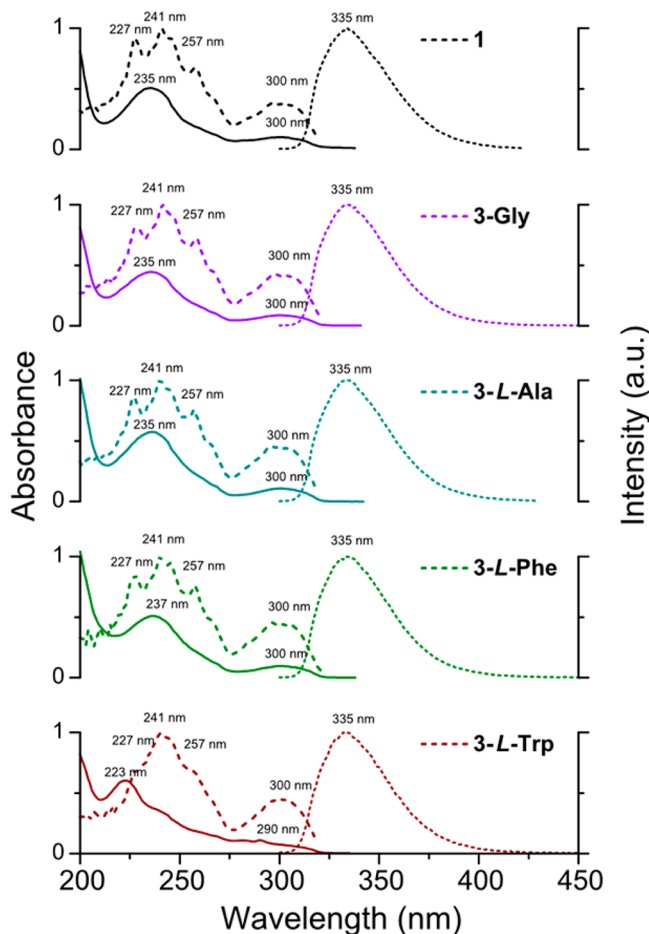


Figure 2. UV–vis absorption, excitation and fluorescence spectra of ligands **1**, **3-Gly**, **3-L-Ala**, **3-L-Phe**, and **3-L-Trp** in CH_3CN solution at 23 °C (the spectra of **3-D-Ala**, **3-D-Phe**, and **3-D-Trp** are shown in Supporting Information).

Table 1. Calculated and Experimental HRMS (MALDI+) Signals for the Various Ln(III) Complexes of Ligands 1 and 3

complex	calculated m/z	experimental m/z , MALDI+
[Eu(1) ₃](CF ₃ SO ₃) ₂ ⁺	1978.369	1978.378
[Eu(3-Gly) ₃](CF ₃ SO ₃) ₂ ⁺	2320.498	2320.489
[Eu(3-L-Ala) ₃](CF ₃ SO ₃) ₂ ⁺	2404.591	2404.599
[Eu(3-D-Ala) ₃](CF ₃ SO ₃) ₂ ⁺	2404.591	2404.571
[Eu(3-L-Phe) ₃](CF ₃ SO ₃) ₂ ⁺	2860.779	2860.783
[Eu(3-D-Phe) ₃](CF ₃ SO ₃) ₂ ⁺	2860.779	2860.787
[Eu(3-L-Trp) ₃](CF ₃ SO ₃) ₂ ⁺	3094.845	3094.852
[Eu(3-D-Phe) ₃](CF ₃ SO ₃) ₂ ⁺	3094.845	3094.860
[Tb(1) ₃](CF ₃ SO ₃) ₂ ⁺	1984.373	1984.370
[Tb(3-Gly) ₃](CF ₃ SO ₃) ₂ ⁺	2326.502	2326.509
[Tb(3-L-Ala) ₃](CF ₃ SO ₃) ₂ ⁺	2410.596	2410.602
[Tb(3-D-Ala) ₃](CF ₃ SO ₃) ₂ ⁺	2410.596	2410.602
[Tb(3-L-Phe) ₃](CF ₃ SO ₃) ₂ ⁺	2866.783	2866.784
[Tb(3-D-Phe) ₃](CF ₃ SO ₃) ₂ ⁺	2866.783	2866.773
[Tb(3-L-Trp) ₃](CF ₃ SO ₃) ₂ ⁺	3100.849	3100.842
[Tb(3-D-Trp) ₃](CF ₃ SO ₃) ₂ ⁺	3100.849	3100.862

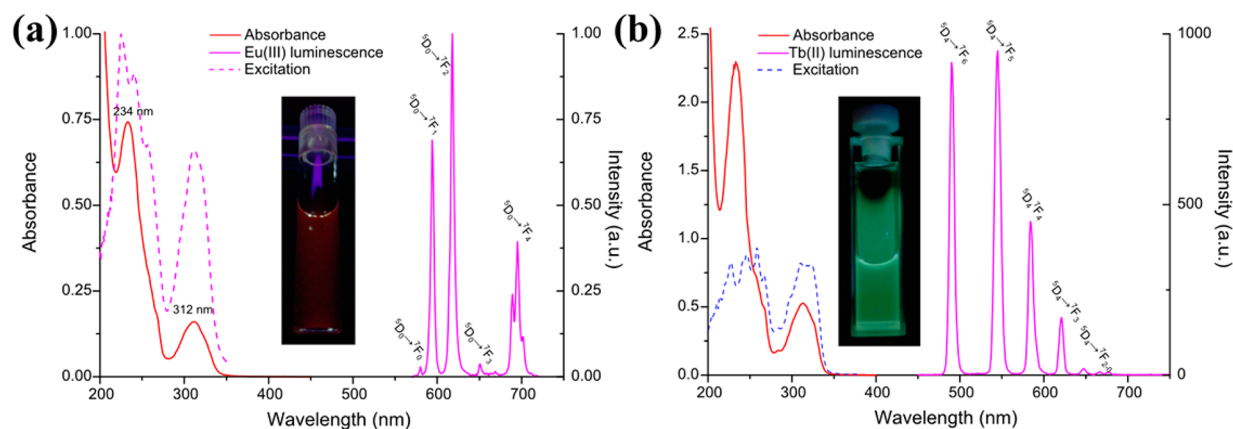


Figure 3. (a) UV-vis absorption (red), sensitized Eu(III) luminescence (magenta), and excitation spectra (dashed magenta) of [Eu(3-L-Phe)₃](CF₃SO₃)₃ in CH₃CN; (b) UV-vis absorption (red), sensitized Tb(III) luminescence (magenta), and excitation spectrum (dashed blue) of [Tb(1)₃](CF₃SO₃)₃ in CH₃CN; insets: photographs of the complex solutions under UV irradiation, showing characteristic visible emission.

In our previous work,^{34–36,39,56–58} we have shown that acyclic ligands based on the **dpa** motif, which have been derivatized with chiral chromophores as antennae, can give rise to sensitized Ln(III) polarized emission, upon complexation with visibly emitting Ln(III) ions and subsequent excitation of the antennae. This we have demonstrated by using circularly polarized luminescence (CPL) spectroscopy, by observing the chiroptical emission of Sm(III), Tb(III), and Eu(III), where such enantiomerically pure complexes give rise to spectra that are mirror images with opposite signs for the various transitions. Similarly, other researchers have demonstrated the same for either cyclic or acyclic ligands.^{59–66} As all of the ligands presented here (except **3-Gly**) possess chiral amino acids adjacent to phenyl antennae, we attempted to record the CPL spectra of these complexes. However, they only gave low intensity CPL spectra for the Ln(III)-centered emission, the best results being observed for [Tb(3-L-Trp)₃](CF₃SO₃)₃ and [Tb(3-D-Trp)₃](CF₃SO₃)₃, showing only very weak signals (see Supporting Information), sufficient only to confirm these complexes were formed as a pair of enantiomers. Unlike the aforementioned complexes, where the chiral antennae were close to the Ln(III) ion, giving rise to strong CPL emission, in the case of the complexes reported here, the chirality of the

amino acid side chain seems to be too remote from the binding site to have any significant impact on the nature of the complex and hence the CPL signal observed.

In order to further understand the energy transfer process of the Ln(III) complexes, the energy levels of the relevant excited states of ligand **1** (singlet and triplet states) were determined. The energy of S₁ (singlet state) was estimated by considering the ligand fluorescence emission with an emission band ranging from 300–420 nm with a maximum at 335 nm (*vide supra*), indicating an energy of ~32 800 cm⁻¹. Since the energy level of T₁ (triplet state) is insensitive to the identity of Ln(III), a complex with Gd(III) was prepared, as described above for the other complexes. The lowest lying excited level of Gd(III) is located at much higher energy than Eu(III) or Tb(III) and hence organic ligands like **1** tend not to sensitize Gd(III)-centered emission, allowing evaluation of T₁. The phosphorescence spectrum of [Gd(1)₃](CF₃SO₃)₃ in CH₃CN, measured at 77 K, displayed a broad structured emission with maxima at 408, 434, 454, and 464 nm (shown in Supporting Information). The energy of T₁ was determined as ~24 500 cm⁻¹. These results are shown schematically in the energy level diagram in Figure 4, which also shows the simplified energy transfer process leading to sensitization of Ln(III) emission,

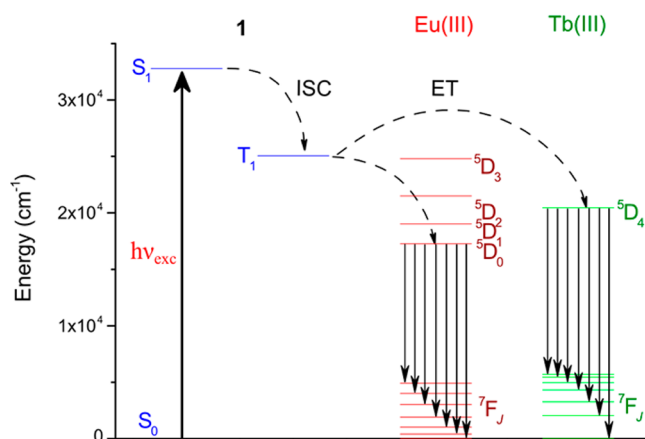


Figure 4. Schematic energy level diagram of the simplified energy transfer processes involved in ligand **1** sensitizing Eu(III)- and Tb(III)-centered luminescence.

occurring via the initial excitation of the S_1 followed by intersystem crossing to T_1 . The energy of T_1 closely matches that of the Eu(III) 5D_0 and Tb(III) 5D_4 states, allowing for energy transfer and population of the Ln(III) excited states.

Analysis of these values show that the energy differences between the triplet energy level of **1**, and the relevant emitting Ln(III)-centered levels were approximately 7000 and 4000 cm^{-1} for Eu(III) and Tb(III) respectively; such a difference is too high to allow effective back energy transfer to either of these systems.⁶⁷ This was further demonstrated by recording the Tb(III) emission in aerated and degassed solution, both of which gave rise to identical spectra, indicating that no quenching by O_2 was observed.⁶⁸ However, the T_1 level is also well positioned to sensitize higher energy states of the Eu(III) 5D_J manifold, which may allow for various nonradiative processes before the $^5D_0 \rightarrow ^7F_J$ transitions occur with associated luminescence, hence the sensitization of the emissive Ln(III) excited state may prove less efficient for Eu(III) than Tb(III) complexes.

Luminescence lifetimes (τ) of these complexes were determined in H_2O and D_2O by fitting the Ln(III) excited state decay profiles of the most intense Ln(III) transitions (the $^5D_0 \rightarrow ^7F_2$ band centered at 616 nm for Eu(III), and the $^5D_4 \rightarrow ^7F_6$ band centered at 490 nm for Tb(III), respectively). These were best fitted to monoexponential decay, Table 2, but the

measurements were carried out at low concentration (10^{-5} M) due to solubility problems at higher concentrations in aqueous media. For both ranges of complexes, the **3-Ala** complexes possessed the longest lifetimes in aqueous environment, with $\tau = 2.71 \pm 0.01$ ms and 2.83 ± 0.02 ms in H_2O and D_2O , respectively, for $[Eu\cdot(3-L-Ala)_3](CF_3SO_3)_3$, while the Eu(III) complex of **1** gave $\tau = 1.06 \pm 0.05$ ms and 1.98 ± 0.01 ms in the same solvents. For the Tb(III) complexes, the lifetimes were generally shorter, with $[Tb\cdot(3-D-Ala)_3](CF_3SO_3)_3$ displaying lifetimes of 1.68 ± 0.08 ms and 1.65 ± 0.03 ms in H_2O and D_2O , respectively, and the complex with **1** giving lifetimes of $\tau = 0.81 \pm 0.14$ ms and 0.85 ± 0.28 ms in the same solvents. These values are similar to those commonly seen for **dpa** based ligands. These data were next used to determine hydration states of these complexes, q , by utilizing the Parker-modified Horrocks equation.^{69,70} As can be seen from Table 2, all the complexes seem to be coordinatively saturated; indicating the successful formation of 1:3 (metal:ligand) complexes as the dominant (or the only) stoichiometry, where the hydration state is ~ 0 . Here, each of the ligands can act as terdentate ligands, giving a total coordination of nine around the Ln(III) ions with no metal bound water molecules.

The luminescence quantum yields, Φ , were also measured for the Eu(III)- and Tb(III)-centered emission by a relative method, by comparison to secondary standards $Cs_3[Ln\cdot(dpa)_3]$ in CH_3CN , Table 2.^{71,72} The quantum yields of the Eu(III) complexes with **1** and **3** were very modest, ranging from 2.1–3.0% for the Gly, Ala, and Phe derivatives. Ligands **3-Trp** were significantly lower (<0.5%), most likely because the Trp antenna is a poor sensitizer for Eu(III). These results demonstrate that these 1:3 complexes possess comparable photophysical properties to those seen for 1:3 complexes formed from the **dpa** systems.^{56,59,74} To our surprise, however, the quantum yields of the Tb(III) complexes were much higher, Table 2, ranging between 6.3–70% in CH_3CN (with the Trp derivatives, once again, being much less bright than the rest of the systems). These quantum yields are comparable to those seen for bis(tetrazolate)pyridyl systems reported by Mazzanti and co-workers.^{47,48} The formation of such highly luminescent complexes can possibly be accounted for by the well matched energy levels for sensitization of the Tb(III) 5D_4 excited state by the **btP** ligands, as discussed above and demonstrated in Figure 4. This marked differential between Tb(III) and Eu(III) complex quantum yields is in contrast to **dpa** systems. To further investigate the structure of these

Table 2. Photophysical Properties of Ln(III) Complexes of Ligands **1** and **3**: Luminescence Lifetimes, Hydration States, and Total Quantum Yields in CH_3CN

ligand	$[Eu\cdot(L)_3](CF_3SO_3)_3$				$[Tb\cdot(L)_3](CF_3SO_3)_3$			
	τ_{H_2O} (ms)	τ_{D_2O} (ms)	q^a (± 0.5)	Φ^b (%)	τ_{H_2O} (ms)	τ_{D_2O} (ms)	q^a (± 0.5)	Φ^b (%)
1	1.06 ± 0.05	1.98 ± 0.01	0.2	2.4 ± 0.4	0.81 ± 0.14	0.85 ± 0.28	-0.5	70 ± 12
3-Gly	1.17 ± 0.39	1.81 ± 0.04	0.1	3.0 ± 0.5	1.26 ± 0.27	1.48 ± 0.12	0.3	53 ± 9
3-L-Ala	2.71 ± 0.01	2.83 ± 0.02	-0.3	2.2 ± 0.4	1.66 ± 0.04	1.64 ± 0.01	-0.3	54 ± 10
3-D-Ala	2.80 ± 0.05	2.78 ± 0.10	-0.3	2.1 ± 0.4	1.68 ± 0.08	1.65 ± 0.03	-0.4	57 ± 10
3-L-Phe	2.31 ± 0.04	2.28 ± 0.01	-0.3	2.2 ± 0.4	1.23 ± 0.01	1.25 ± 0.01	-0.2	61 ± 11
3-D-Phe	2.65 ± 0.05	2.72 ± 0.01	-0.3	2.5 ± 0.4	1.24 ± 0.03	1.23 ± 0.03	-0.3	46 ± 8
3-L-Trp	1.07 ± 0.04	1.38 ± 0.05	-0.1	0.3 ± 0.1	0.76 ± 0.02	0.85 ± 0.01	0.4	11 ± 2
3-D-Trp	0.68 ± 0.03	1.25 ± 0.10	0.5	0.4 ± 0.1	0.83 ± 0.01	0.84 ± 0.01	-0.3	6.3 ± 1.1

^aHydration states were calculated using the equation $q = A((1/\tau_{H_2O} - 1/\tau_{D_2O}) - B)$, where for Eu(III), $A = 1.2$, $B = 0.25$ and for Tb(III), $A = 5.0$, $B = 0.06$.^{31,70} ^bQuantum yields in CH_3CN were estimated by a relative method,^{71,72} compared with $Cs_3[Ln\cdot(dpa)_3]$ ⁷³ according to the equations shown in Supporting Information.

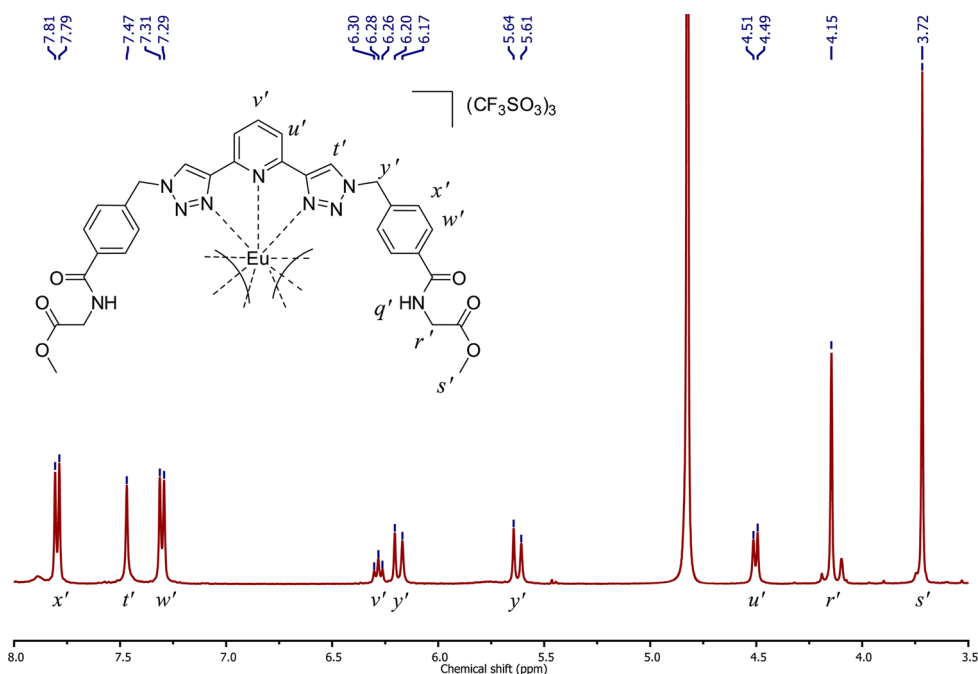


Figure 5. ^1H NMR spectrum (400 MHz, CD_3OD) of $[\text{Eu}\cdot(3\text{-Gly})_3](\text{CF}_3\text{SO}_3)_3$, showing paramagnetically shifted resonances, compared to the ligand spectrum.

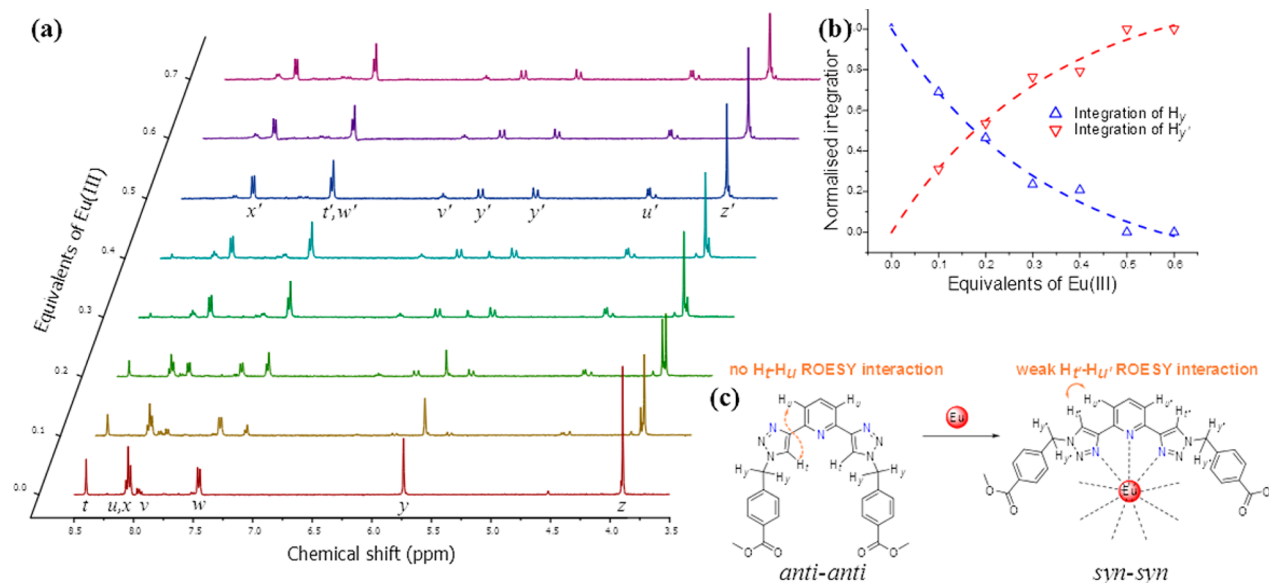


Figure 6. (a) ^1H NMR (400 MHz, CD_3CN) titration of ligand **1** upon addition of $\text{Eu}(\text{CF}_3\text{SO}_3)_3$ solution; (b) a graph showing ratios of the integrations of the methylene resonances (labeled γ) of each species as a function of equivalents of $\text{Eu}(\text{III})$ added; (c) schematic representation of the interconversion between *anti-anti* and *syn-syn* conformation of **1** upon complexation.

complexes, we carried out ^1H NMR analysis of **1** with $\text{Eu}(\text{III})$ in CD_3CN .

^1H NMR Studies of Ligand **1 upon Titration with $\text{Eu}(\text{III})$.** The ^1H NMR spectra of $\text{Ln}(\text{III})$ complexes are often very difficult to interpret as a result of the paramagnetic nature of many of the $\text{Ln}(\text{III})$ ions, including $\text{Eu}(\text{III})$ and $\text{Tb}(\text{III})$, which can broaden and shift proton resonances, sometimes beyond recognition. In the case of some of the $\text{Eu}(\text{III})$ complexes with ligands **1** and **3**, the spectra were relatively well resolved, albeit paramagnetically shifted, particularly those resonances close to the **bt**p binding motif. The spectrum (400 MHz, CD_3OD) of $[\text{Eu}\cdot(3\text{-Gly})_3](\text{CF}_3\text{SO}_3)_3$ is shown in

Figure 5 as an example, with the various peaks labeled. Most notable shifts to lower frequency were seen for pyridyl (labeled u' and v') and triazolyl (labeled t') proton resonances, with the 3- and 5-pyridyl signal appearing at a chemical shift where aliphatic protons are usually observed. The fact that the dipolar shift in proton resonances is minor compared to other $\text{Eu}(\text{III})$ complexes corresponds with the very small splitting observed in the $^5\text{D}_0 \rightarrow ^7\text{F}_1$ transitions; correlation between these parameters was described in recent work by Parker and co-workers.^{75,76}

In light of the fact that the complex ^1H NMR spectra differ significantly from the ligand spectra, titrations were undertaken

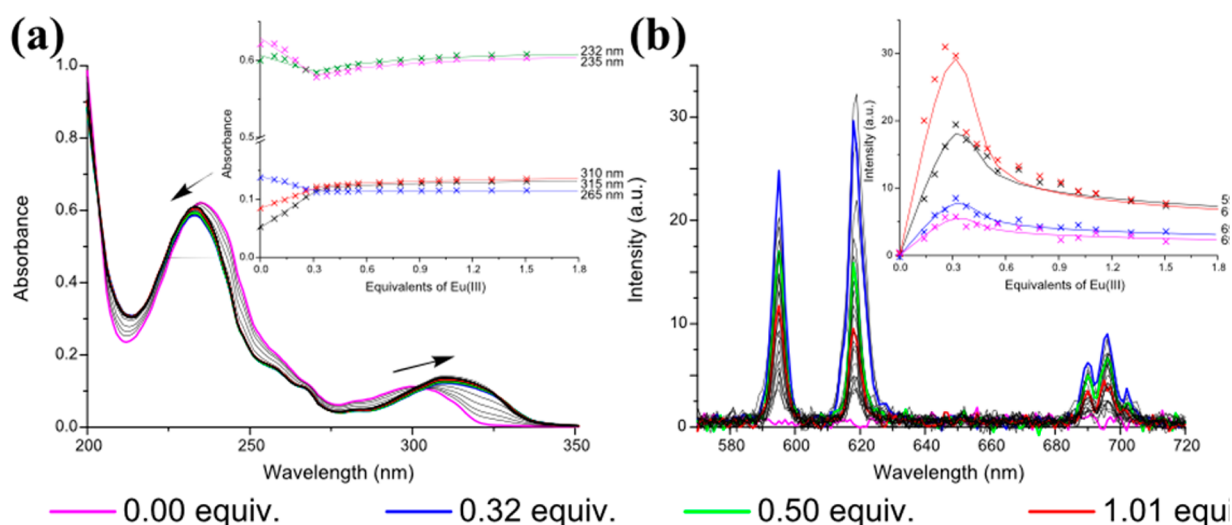


Figure 7. Titration plots of **1** v. Eu(III) in CH₃CN. (a) UV-vis spectral changes; inset: experimental binding isotherms (×) and calculated isotherms (solid lines) at various wavelengths; (b) changes in Eu(III) luminescence; inset: experimental binding isotherms (×) and calculated isotherms (solid lines) at various wavelengths. Fluorescence spectral changes are shown in Supporting Information.

to observe the changes in the spectrum of ligand **1**, and the different self-assembly species formed in a solution of CD₃CN as a function of [Eu(III)] with a view to understanding the geometry of the free ligand, as compared with the coordinating ligand.

As shown in Figure 6a, the changes in the NMR spectra were in slow exchange on the NMR time scale, the most significant changes occurring within the addition of 0.0 → 0.5 equiv of Eu(III), followed thereafter by increased broadening and complexity of signals. The resonance arising from the methyl ester resonance in **1** (3.86 ppm, labeled *z*) underwent a slight shift to higher frequency upon self-assembly, with the free ligand signal disappearing completely by the addition of 0.5 equiv and being replaced by a signal at 3.89 ppm (labeled *z'*). Concomitantly, shifts were observed in the aromatic region. Most significant among these was the disappearance of the triazolyl resonance at 8.40 ppm (*t*) upon addition of 0.5 equiv of Eu(III); this resonance was determined by 2D NMR spectroscopy (see Supporting Information) to overlap with one of the phenyl CH signals at 7.23 ppm in the complex (*t'*). The triplet pertaining the 4-pyridyl proton showed a significant paramagnetic shift from 7.91 ppm (*v*) to 6.27 ppm (*v'*), an exchange which was also complete by 0.5 equiv; the 3- and 5-pyridyl proton signal (*u*) shifted dramatically to lower frequency as well, but this is less clearly monitored as a result of the ligand peak overlapping with one of the phenyl proton signals, only becoming clearly resolved as a doublet (labeled *u'*) at 4.54 ppm upon complexation (confirmed by selective ROESY and HSQC, see Supporting Information). The phenyl protons (*w* and *x*) also became more shielded, but less notably so. These kinds of pyridyl shifts to lower frequency are similar to those reported for **dpa** based ligands previously.⁷⁷ Interestingly, the CH₂ signal at 5.7 ppm (*y*) split into two doublets upon complexation; this would suggest a locking of the ligand “arms” into a conformation where free rotation of this bond is no longer possible. Figure 6b shows the interconversion of these two signals by representing the relative integrations of the resonances marked *y* and *y'* as a function of equivalents of Eu(III) added.

Through the use of selective ROESY experiments (shown in Supporting Information), information about the spatial

conformation of the free ligand and the ligand as part of the complex was obtained. Consistent with the *anti-anti* structure seen in the crystal structure of **1**, which we have previously published,²⁰ the triazolyl proton did not show any through-space interactions with the 3-pyridyl protons. This “horseshoe” conformation was similar to that seen by other similar compounds in the literature.^{2,9,22,23,78} Upon addition of 0.5 equiv of Eu(III), however, the new species showed weak interactions between the 3-pyridyl protons and the triazolyl resonance, consistent with the inversion of triazolyl conformation in the **btp** motif to *syn-syn* geometry (as schematically represented in Figure 6c), as has been previously reported for similar systems, resulting from the nitrogen lone-pairs binding the metal ion.¹⁰

Having shown the competency of **btp** ligands for binding Ln(III) ions through formation of emissive thermal complexes and monitoring the self-assembly of **1** with Eu(III) in CD₃CN by ¹H NMR spectroscopy, more detailed investigations of this self-assembly were carried out in CH₃CN by monitoring the changes in the UV-vis absorption, fluorescence, and Ln(III) luminescence spectra upon addition of Eu(III) or Tb(III) triflate salt solution to ligand solutions at concentrations of ca. 10⁻⁵ M (accurate concentrations were determined using the Beer-Lambert Law).

Observing Ln(III)-Directed Self-Assembly Formation through Photophysical Studies. The ligands developed herein were titrated with both Eu(III) and Tb(III) triflate. The overall changes in the absorption spectrum of a CH₃CN solution of **1** were monitored as a function of [Eu(III)], Figure 7. A slight blue shift and concomitant decrease in absorbance was observed for the peak at 235 nm, stabilizing at 232 nm, while the other peak, centered at 300 nm, and assigned to **btp** n → π* transitions, underwent a more significant red shift of 15 nm with an increase in absorbance. Coordination of the metal ion by the **btp** motif accounts for this notable change. The spectra after these changes match the recorded spectra of the thermally prepared metal complex. Experimental binding isotherms at various wavelengths are shown as an inset in Figure 7a, demonstrating that changes to the absorption spectra were largely finished upon addition of approximately 0.33 equiv of Eu(CF₃SO₃)₃, signifying the formation of the desired 1:3

Table 3. Binding Constants Determined from Titrations of **btp** Ligands with Ln(III) in CH₃CN^a

ligand		Eu(III)			Tb(III)			
		logβ _{1:1}	logβ _{1:2}	logβ _{1:3}	logβ _{1:1}	logβ _{1:2}	logβ _{1:3}	
1	UV	6.0 ± 0.1	13.0 ^b	19.8 ^b	UV	6.5 ^b	13.0 ^b	18.9 ± 0.1
	Fluor.	6.9 ^b		22.2 ± 0.1	Fluor.			
	Lum.	7.2 ± 0.1	14.8 ^b	20.7 ^b	Lum.	6.9 ^b	14.2 ± 0.1	20.2 ± 0.1
3-Gly	UV	6.5 ^b	14.3 ± 0.1	21.2 ^b	UV	6.9 ^b		22.7 ± 0.7
	Lum.	7.3 ± 0.1	15.2 ^b	21.4 ± 0.1	Lum.	6.9 ± 0.14		20.5 ± 0.1
3-L-Ala	UV	8.0 ± 0.1	14.8 ± 0.1	21.8 ± 0.2	UV	7.2 ± 0.14	14.4 ^b	21.6 ± 0.1
	Fluor.	7.4 ^b	14.3 ^b	21.4 ± 0.1	Fluor.	7.2 ^b		22.1 ± 0.1
	Lum.	7.3 ± 0.1	15.2 ^b	21.5 ± 0.1	Lum.	6.9 ± 0.1	14.6 ^b	22.0 ± 0.1
3-D-Ala	UV	7.7 ± 0.1	14.7 ^b	20.1 ± 0.1	UV	6.9 ^b	14.4 ± 0.1	20.0 ± 0.1
	Lum.	8.5 ± 0.1	15.6 ^b	21.7 ± 0.1	Lum.	7.2 ^b	14.6 ± 0.1	20.7 ± 0.1
3-L-Phe	UV	7.1 ± 0.1	14.9 ^b	21.2 ± 0.1	UV	7.28 ^b	14.6 ^b	20.9 ± 0.1
	Lum.	7.9 ± 0.1	16.3 ^b	21.0 ^b	Lum.	7.3 ^b	15.2 ^b	21.6 ± 0.1
3-D-Phe	UV	7.1 ^b	14.6 ^b	21.5 ± 0.1	UV	7.6 ± 0.1	14.9 ^b	20.4 ± 0.1
	Lum.	8.5 ± 0.2	17.3 ± 0.3	23.0 ± 0.4	Lum.	6.8 ± 0.1	15.1 ± 0.1	21.4 ± 0.2
3-L-Trp	UV	6.6 ^b	14.2 ^b	20.2 ± 0.1	UV	6.8 ^b	14.7 ^b	21.4 ± 0.1
	Fluor.				Fluor.	6.8 ^b	14.9 ± 0.1	20.4 ^b
	Lum.	7.7 ^b	14.9 ± 0.1	19.7 ^b	Lum.	6.8 ^b	15.0 ^b	21.7 ± 0.1
3-D-Trp	UV	6.6 ± 0.1	14.2 ± 0.2	20.7 ± 0.3	UV	6.8 ± 0.2	14.9 ± 0.3	21.3 ± 0.4
	Fluor.	7.7 ^b	16.8 ± 0.1	23.7 ^b	Fluor.			
	Lum.	7.7 ± 0.1	14.6 ± 0.1	19.8 ± 0.1	Phos.	6.8 ^b	16.2 ± 0.2	21.3 ^b

^a[L] ≈ 10⁻⁵ M. ^bValue fixed.

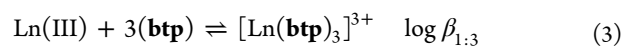
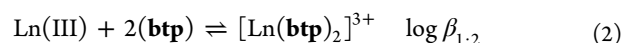
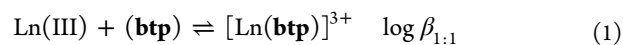
complex. The changes in fluorescence emission spectra were also recorded, with the ligand fluorescence centered at 335 nm being quenched upon addition of 0.33 equiv also. The concomitant emergence of Eu(III) luminescence emission was monitored by recording the delayed Ln(III) emission (phosphorescence) upon excitation of the ligand. The overall changes in the Eu(III) emission profile are shown in Figure 7b, demonstrating gradual enhancement of the characteristic Eu(III) luminescence spectrum within the addition of 0–0.33 equiv of metal ion, signifying both the successful sensitization of the lanthanide excited state and the successful formation of the Eu(III)-directed self-assembly in solution. The inset in Figure 7b shows the changes observed over the course of the titration for various ⁵D₀ → ⁷F_J transitions; it is clear from these changes that after the addition of 0.33 equiv of Eu(III), a sharp decrease in the Eu(III)-centered emission was observed, an indication of the formation of other self-assemblies in solution, and that this shift in equilibrium causes the formation of less emissive species to become the most dominant species in solution. This is similar to behavior often observed for **dpa** based ligands, and has been, in those cases, assigned to the formation of 1:2 and 1:1 stoichiometries.

Analogous spectroscopic changes for ligands **3** are discussed in detail in Supporting Information. The changes observed for ligands **3-Trp** are, however, worth commenting on here, as these possessed more complicated absorption spectra to those seen above, as the Trp residues give rise to some distinctive absorption bands not seen in the aforementioned ligands (see Supporting Information). The Trp-based band centered at 290 nm decreased in intensity upon addition of metal ion until 0.5 equiv, while the shoulder centered at 236 nm disappeared altogether. Simultaneously, the band centered at 232 nm decreased in intensity as a function of added Eu(III), whereas a band centered at 315 nm grew in absorbance. The fluorescence emission was also quenched upon binding to Eu(III), these changes being most pronounced up to the addition of 0.5 equiv. As seen above, the Eu(III)-centered luminescence

peaked at 0.33 equiv and was subsequently quenched after the addition of 1.0 equiv of Eu(III), indicating that the 1:3 stoichiometry was the most emissive species, as was the case for all ligands discussed thus far. These ligands were not very efficient, however, at sensitizing Eu(III) luminescence, as can be seen from the poor resolution of the phosphorescence spectra and from the quantum yield measurements detailed above. The results observed for the other ligands developed herein upon titration with Eu(III) are shown in Supporting Information.

Similarly, we evaluated the changes in the various spectroscopic properties of these ligands upon titrating with Tb(III). The results yielded very similar trends to those seen from the above titrations and are discussed in Supporting Information.

Quantifying the Binding Affinity and Speciation Distribution through Photophysical Studies. In order to gain a better understanding of this solution self-assembly behavior and obtain a more detailed view on the formation of different stoichiometric species in solution, the various spectroscopic changes determined in the above measurements were analyzed by fitting the global changes using nonlinear regression analysis (using the ReactLab Equilibria software⁷⁹) to various **btp**:Ln(III) stoichiometries and stability constants (logβ) for each equilibrium were determined. Global stability constants were estimated for all ligands, **1** and **3**, with Eu(III) and Tb(III) from the UV–vis absorbance and Ln(III) luminescence studies, while for some ligands, it was possible to estimate values from ligand fluorescence titration data as well, using the following equilibrium processes:



Across the series of ligands, the estimated values of equilibrium constants were of similar magnitude (as shown in Table 3) with $\log\beta_{1:1}$ ranging from 6.0–8.5, $\log\beta_{1:2}$ of 14.2–17.3 and $\log\beta_{1:3}$ of 19.8–23.7, although in some cases values of $\log\beta_{1:2}$ could not be determined. In all but one case, the constants estimated from Ln(III)-centered measurements were higher than those determined from the absorption data.

The binding constants with Ln(III) were in good agreement with the range of values reported for similar compounds in the literature and at the upper end of the reported range,^{56,59,74,80,48} suggesting that these ligands are capable of forming very stable coordination compounds with Ln(III) in CH₃CN solution.

The calculated speciation distribution diagrams for these titrations are shown in Supporting Information. These demonstrated that for all the titrations, the 1:3 stoichiometry was initially formed in high yield, (for instance, in the case of **1** with Eu(III), in ca. 85% yield) after which the formation of the 1:2 species became apparent (in all but a few cases), eventually followed by the formation of the 1:1 complex at higher Ln(III) concentrations. This kind of behavior is similar to that seen in our work using **dpa** derivatives, demonstrating the similar coordination properties of the two systems. Hence, the results demonstrate that amino acid conjugated **btp** ligands can be used to form novel self-assembly structures where the final assembly contains 6, 4, or 2 such monopeptide conjugates. Since all of these are based on methyl esters, they can be further modified, with a view to achieving better solubility in aqueous solution, or with the objective of forming higher order self-assemblies and novel materials (such as gels) for instance by simple hydrolysis and interactions with metal ions; an endeavor that is currently being pursued in our laboratory with a view to forming novel functional MOFs and soft materials.

CONCLUSIONS

In the work presented in this article, we have developed seven new **btp** ligands, **3** (derived from previously reported ligand **1**), their synthesis and characterization being discussed in detail for a select number of them. All the ligands contained amino acid residues, which were incorporated at the aryl terminal of these ligands, enabling further functionalization of these moieties in the future. Ligands **1** and **3** all formed stable, luminescent complexes with Ln(III) salts, displaying characteristic Eu(III) or Tb(III) line-like emission profiles upon sensitization via the “antenna effect”. A hydration state of $q \approx 0$ was determined for each complex, indicating the absence of water molecules bound in the first coordination sphere of the metal ion and the ability of these ligands to satisfy the high coordination requirements of Ln(III). Of these the Tb(III) complexes were shown to be highly luminescent with quantum yield for the metal centered emission being determined to be within the range of 46–70%, with the exception of Trp derivatives which were significantly less luminescent. The Eu(III) complexes were much less luminescent, with a quantum yield of 0.3–3%, reflecting less efficient sensitization process; this we analyzed by measuring the triplet state of the ligand **1**. As in the case of Tb(III) the Trp derivatives of Eu(III) were the least emissive. The interactions of ligand **1** with Eu(III) ions in CD₃CN were studied through NMR studies, showing that the **btp** motif can bind this metal ion, forming a stable 1:3 self-assembly, which was also confirmed by HRMS analysis. Spectroscopic titrations of **1** and **3** with Eu(III) and Tb(III) were carried out in CH₃CN solution in order to monitor the self-assembly behavior of these ligands in solution. The stability constants of the various self-

assembled species were high, and comparable to **dpa** based derivatives previously developed in our laboratory, as well as other terdentate systems in the literature; these varied very little throughout the series of compounds. The study herein demonstrates that the **btp** ligands are a useful addition to the chemistry of the lanthanides, possessing three coordination sites that can be used in the formation of highly ordered self-assemblies, which can exist in 1:3, 1:2, or 1:1 stoichiometries. We have further shown that these can be simply functionalized by using classical organic chemistry and, as such, the **btp** ligands are excellent candidates for developing novel structures and functional Ln(III)-based materials. We are currently working toward exploring the use of **btp** derivatives in greater detail for such applications.

EXPERIMENTAL SECTION

Methods and Materials. All chemicals were purchased from commercial sources and, unless specified, used without further purification. Melting points were determined using an Electrothermal IA9000 digital melting point apparatus. Elemental analysis was carried out at the Microanalytical Laboratory, School of Chemistry and Chemical Biology, University College Dublin using an Exeter Analytical CE 440 elemental analyzer. Infrared spectra were recorded on a PerkinElmer Spectrum One FT-IR Spectrometer fitted with a universal ATR sampling accessory. NMR spectra were recorded using a Bruker DPX-400 Avance spectrometer or Agilent DD2/LH spectrometer, operating at 400.13 MHz for ¹H NMR, 100.6 MHz for ¹³C NMR, or a Bruker AV-600 spectrometer, operating at 600.1 MHz for ¹H NMR and 150.2 MHz for ¹³C NMR. All spectra were recorded using commercially available deuterated solvents, and were referenced to solvent residual proton signals. All ¹H–¹H coupling constants, *J*, are quoted with an accuracy of ±0.3 Hz. Electrospray mass spectra were measured on a Micromass LCT spectrometer calibrated using a leucine enkephaline standard. MALDI Q-ToF mass spectra were carried out on a MALDI Q-ToF Premier (Waters Corporation, Micromass MS technologies, Manchester, UK) and high-resolution mass spectrometry was performed using Glu-Fib as an internal reference (peak at *m/z* = 1570.677). All microwave reactions were carried out in 2–5 mL or 10–20 mL Biotage Microwave Vials in a Biotage Initiator Eight EXP microwave reactor. Ligands **1** and **2** were prepared as previously reported.²⁰

Photophysical Measurements. Unless otherwise stated, all photophysical measurements were carried out at 23 °C in HPLC CH₃CN solution at a concentration of ca. 10⁻⁵ M. UV–visible absorption spectra were measured in 1 cm quartz cuvettes on a Varian Cary 50 spectrophotometer. Baseline correction was applied for all spectra. Emission spectra and luminescence lifetimes were measured on a Varian Cary Eclipse luminescence spectrometer. All the stock solutions were prepared in CH₃CN. Low temperature emission spectra were recorded on a Fluorolog FL-3-22 spectrometer from Horiba-Jobin-Yvon Ltd. This instrument was equipped with a dewar of liquid nitrogen, allowing for measurements at 77 K.

Sample Procedure for Synthesis of Amino-Acid Derivative, 3-Gly. Ligand **2** (0.20 g, 0.42 mmol) was suspended in 4 mL of SOCl₂ and heated to 80 °C for 18 h under a CaCl₂ guard tube. SOCl₂ was removed by vacuum distillation, and the acid chloride was suspended in distilled CH₂Cl₂ and used without further purification. In a separate reaction vessel, the relevant amino acid methyl ester HCl salt (3.3 equiv) was suspended in distilled CH₂Cl₂ and stirred for 1 h with an excess of triethylamine (0.2 mL) at room temperature. The two suspensions were added together and stirred at room temperature for 18 h under a CaCl₂ guard tube. The reaction mixture was concentrated under reduced pressure. The product was isolated upon trituration with CH₃OH and collected by filtration, washing with CH₃OH and diethyl ether, yielding the amide as a white or off-white solid.

Yield: 51%. Mp: 136–141 °C. HRMS (*m/z*) (ESI⁺): Calculated for C₃₁H₃₀N₉O₆⁺ *m/z* = 624.2319 [M + H]⁺. Found *m/z* = 624.2308; calculated for C₃₁H₂₉N₉O₆·0.75NaCl·0.75H₂O, C = 54.68, H = 4.51, N

= 18.51. Found C = 55.02, H = 4.11, N = 18.45; ^1H NMR (600 MHz, DMSO- d_6): δ (ppm) = 3.65 (s, 6H, COOCH₃), 4.02 (d, 4H, CH₂, J = 5.8 Hz), 5.79 (s, 4H, CH₂), 7.46 (d, 4H, Ph CH, J = 8.0 Hz), 7.89 (d, 4H, Ph CH, J = 8.0 Hz), 7.93–8.05 (m, 3H, pyr CH), 8.72 (s, 2H, triazolyl CH), 8.97 (t, 2H, NH, J = 5.8 Hz); ^{13}C NMR (150 MHz, DMSO- d_6): δ (ppm) = 41.5 (Gly CH), 52.1 (CH₃), 53.0 (CH₂), 118.9 (pyr CH), 124.1 (triazolyl CH), 128.1 (Ph CH), 128.2 (Ph CH), 133.8 (Ph qt), 138.6 (pyr CH), 139.6 (Ph qt), 147.7 (triazolyl qt), 150.1 (pyr qt), 166.5 (amide C=O), 170.6 (ester C=O); FT-IR (ATR, cm⁻¹): 3339, 3079, 2956, 2285, 2167, 2080, 1981, 1740, 1645, 1615, 1575, 1544, 1505, 1436, 1402, 1371, 1321, 1303, 1263, 1212, 1160, 1115, 1095, 1052, 1020, 993, 979, 803, 765, 732, 694, 663.

3-*L*-Ala. Yield: 57%. Mp: 253–254 °C. HRMS (m/z) (ESI+): Calculated for C₃₃H₃₄N₉O₆⁺ m/z = 652.2632 [M + H]⁺. Found m/z = 652.2653; calculated for C₃₃H₃₃N₉O₆·H₂O, C = 59.19, H = 5.27 N = 18.82. Found C = 58.86, H = 4.86 N = 18.88; ^1H NMR (600 MHz, DMSO- d_6): δ (ppm) = 1.40 (d, 6H, Ala CH₃, J = 7.2 Hz), 3.64 (s, 6H, COOCH₃), 4.48 (quin, 2H, Ala CH, J = 7.2 Hz), 5.79 (s, 4H, CH₂), 7.46 (d, 4H, phenyl CH, J = 8.1 Hz), 7.91 (d, 4H, phenyl CH, J = 8.1 Hz), 7.99 (app s, 3H, pyridyl CH), 8.71 (s, 2H, triazolyl CH), 8.81 (d, 2H, NH, J = 7.0 Hz); ^{13}C NMR (150 MHz, DMSO- d_6): δ (ppm) = 17.0, 48.6 (Ala CH), 52.2 (COOCH₃), 53.0 (CH₂), 118.9 (pyr CH), 124.0 (triazolyl CH), 128.1 (Ph CH), 128.3 (Ph CH), 133.9 (qt), 138.6 (pyr CH), 139.5 (qt), 147.7 (qt), 150.1 (qt), 166.1 (qt), 173.4 (qt); FT-IR (ATR, cm⁻¹): 3353, 3169, 2957, 2162, 2050, 1741, 1642, 1609, 1577, 1532, 1505, 1459, 1438, 1426, 1380, 1359, 1320, 1271, 1238, 1212, 1198, 1167, 1096, 1080, 1045, 1021, 993, 980, 939, 876, 849, 801, 790, 776, 759, 742, 660.

3-*D*-Ala. Yield: 48%. Mp: 254–255 °C. HRMS (m/z) (ESI+): Calculated for C₃₃H₃₄N₉O₆⁺ m/z = 652.2632 [M + H]⁺. Found m/z = 652.2635; calculated for C₃₃H₃₃N₉O₆·NaCl·0.5H₂O, C = 55.63, H = 4.38, N = 17.64. Found C = 55.46, H = 4.73, N = 17.64; ^1H NMR (600 MHz, DMSO- d_6): δ (ppm) = 1.40 (d, 6H, Ala CH₃, J = 7.3 Hz), 3.64 (s, 6H, COOCH₃), 4.48 (quin, 2H, Ala CH, J = 7.2 Hz), 5.79 (s, 4H, CH₂), 7.46 (d, 4H, phenyl CH, J = 8.2 Hz), 7.91 (d, 4H, phenyl CH, J = 8.3 Hz), 7.94–8.06 (m, 3H, pyridyl CH), 8.71 (s, 2H, triazolyl CH), 8.81 (d, 2H, NH, J = 7.0 Hz); ^{13}C NMR (150 MHz, DMSO- d_6): δ (ppm) = 16.8, 48.2 (Ala CH), 51.8 (COOCH₃), 52.6 (CH₂), 118.5 (pyr CH), 123.7 (triazolyl CH), 127.7 (phenyl CH), 127.9 (phenyl CH), 133.5 (qt), 138.3 (pyr CH), 139.1 (qt), 147.4 (qt), 149.7 (qt), 165.7 (qt), 173.0 (qt); FT-IR (ATR, cm⁻¹): 3351, 3168, 2957, 2162, 2046, 1741, 1642, 1609, 1577, 1532, 1505, 1460, 1438, 1426, 1380, 1359, 1346, 1315, 1271, 1238, 1212, 1198, 1167, 1135, 1096, 1080, 1045, 1021, 993, 980, 938, 876, 849, 801, 790, 759, 742, 660.

3-*L*-Phe. Yield: 61%. Mp: 139–148 °C. HRMS (m/z) (ESI+): Calculated for C₄₅H₄₁N₉O₆Na⁺ m/z = 826.3078 [M + Na]⁺. Found m/z = 826.3071; calculated for C₄₅H₄₁N₉O₆·0.5NaCl·H₂O, C = 63.50, H = 5.09, N = 14.81. Found C = 64.04, H = 4.84, N = 14.74; ^1H NMR (600 MHz, DMSO- d_6): δ (ppm) = 3.05–3.19 (m, 4H, Phe CH₂), 3.63 (s, 6H, COOCH₃), 4.66 (octet, 2H, Phe CH, J = 3.3 Hz), 5.77 (s, 4H, CH₂), 7.15–7.20 (m, 2H, Phe *p*-Ph CH), 7.25–7.30 (m, 8H, Phe *m*- and *o*-Ph CH), 7.43 (d, 4H, Ph CH adjacent to CH₂, J = 8.3 Hz), 7.82 (d, 4H, phenyl CH adjacent amide bond), 7.96–8.01 (m, 3H, pyr CH), 8.70 (s, 2H, triazolyl CH), 8.86 (d, 2H, NH, J = 7.9 Hz). ^{13}C NMR (150 MHz, DMSO- d_6): δ (ppm) = 36.5 (Phe CH₂), 52.3 (COOCH₃), 53.0 (CH₂), 54.6 (Phe CH), 118.9 (pyr CH), 124.1 (triazolyl CH), 126.8 (Phe *o*-Ph CH), 128.1 (Ph CH), 128.2 (Ph CH), 128.5 (Phe Ph CH), 129.4 (Phe Ph CH), 133.8, 137.9, 138.7 (pyr CH) 139.6, 147.7, 150.1, 166.3, 172.4. FT-IR (ATR, cm⁻¹): 3442, 3375, 3156, 3055, 3031, 2949, 1736, 1639, 1604, 1574, 1524, 1495, 1458, 1436, 1352, 1279, 1217 (s), 1198, 1175, 1152, 1088, 1045, 1021, 992, 977, 921, 864, 803, 736.

3-*D*-Phe. Yield: 47%. Mp: 141–149 °C. HRMS (m/z) (ESI-): Calculated for C₄₅H₄₀N₉O₆⁻ m/z = 802.3107 [M - H]⁻. Found m/z = 802.3115; calculated for C₄₅H₄₁N₉O₆·1.5H₂O, C = 65.05, H = 5.34, N = 15.17. Found C = 64.88, H = 5.08, N = 14.69; ^1H NMR (600 MHz, DMSO- d_6): δ (ppm) = 3.05–3.19 (m, 4H, Phe CH₂), 3.63 (s, 6H, COOCH₃), 4.66 (octet, 2H, Phe CH, J = 3.3 Hz), 5.77 (s, 4H, CH₂), 7.15–7.20 (m, 2H, Phe *p*-Ph CH), 7.25–7.30 (m, 8H, Phe *m*- and *o*-Ph CH), 7.43 (d, 4H, Ph CH adjacent to CH₂, J = 8.3 Hz), 7.81

(d, 4H, Ph CH adjacent amide bond), 7.96–8.01 (m, 3H, pyr CH), 8.70 (s, 2H, triazolyl CH), 8.86 (d, 2H, NH, J = 7.9 Hz). ^{13}C NMR (150 MHz, DMSO- d_6): δ (ppm) = 36.2 (Phe CH₂), 52.0 (COOCH₃), 52.7 (CH₂), 54.3 (Phe CH), 118.6 (pyr CH), 123.8 (triazolyl CH), 126.5 (Phe *o*-Ph CH), 127.8 (Ph CH), 127.9 (Ph CH), 128.2 (Phe Ph CH), 129.0 (Phe Ph CH), 133.5, 137.6, 138.3 (pyr CH) 139.2, 147.4, 149.8, 166.0, 172.1; FT-IR (ATR, cm⁻¹): 3320, 3132, 3055, 3031, 2949, 1736, 1643, 1611, 1575, 1530, 1497, 1456, 1433, 1352, 1279, 1215 (s), 1198, 1175, 1152, 1083, 1043, 1019, 992, 977, 914, 864, 806, 741.

3-*L*-Trp. Yield: 47%. Mp: 170–173 °C. HRMS (m/z) (ESI+): Calculated for C₄₉H₄₃N₁₁O₆Na⁺ m/z = 904.3295 [M + Na]⁺. Found m/z = 904.3250; calculated for C₄₉H₄₃N₁₁O₆·1.25H₂O, C = 65.07, H = 5.07, N = 17.03. Found C = 64.86, H = 4.57, N = 17.09; ^1H NMR (600 MHz, DMSO- d_6): δ (ppm) = 3.22 (dd, 2H, Trp CH₂, J = 9.0 Hz, 14.5 Hz), 3.24 (dd, 2H, Trp CH₂, J = 5.2 Hz, 14.5 Hz), 3.62 (s, 6H, COOCH₃), 4.69 (ddd, 2H, Trp CH, J = 7.4 Hz, 9.0 Hz, 5.2 Hz), 5.77 (s, 4H, CH₂), 6.98 (t, 2H, Trp CH, J = 7.4 Hz), 7.06 (t, 2H, Trp CH, J = 7.4 Hz), 7.19 (d, 2H, Trp CH, J = 2.2 Hz), 7.32 (d, 2H, Trp CH, J = 8.0 Hz), 7.43 (d, 4H, Ph CH, J = 8.3 Hz), 7.55 (d, 2H, Trp CH, J = 7.9 Hz), 7.84 (d, 4H, Ph CH, J = 8.3 Hz), 7.96–8.03 (m, 3H, pyr CH), 8.70 (s, 2H, triazolyl CH), 8.81 (d, 2H, amide NH, J = 7.6 Hz), 10.80 (s, 2H, Trp NH); ^{13}C NMR (150 MHz, DMSO- d_6): δ (ppm) = 26.6 (Trp CH₂), 51.9 (CH₃), 52.6 (CH₂), 53.8 (chiral CH), 109.9 (Trp qt), 111.4 (Trp CH), 118.0 (Trp CH), 118.4 (Trp CH), 118.6 (pyr CH), 121.0 (Trp CH), 123.6 (Trp CH), 123.7 (triazolyl CH), 127.0 (Trp qt), 127.7 (Ph CH), 127.9 (Ph CH), 133.5 (Ph qt), 136.1 (Trp qt), 139.2 (Ph qt), 147.4 (triazolyl qt), 149.8 (pyr qt), 166.0 (amide C=O), 172.4 (ester C=O); FT-IR (ATR, cm⁻¹): 3441, 3387, 3155, 3055, 2953, 1737, 1640, 1611, 1575, 1525, 1497, 1458, 1437, 1346, 1279, 1217, 1196, 1176, 1153, 1089, 1045, 1021, 1012, 992, 977, 930, 865, 803, 766, 735, 673.

3-*D*-Trp. Yield: 60%. Mp: 168–171 °C. HRMS (m/z) (ESI+): Calculated for C₄₉H₄₄N₁₁O₆⁺ m/z = 882.3476 [M + H]⁺. Found m/z = 882.3440; calculated for C₄₉H₄₃N₁₁O₆·0.5NaCl·2H₂O, C = 62.13, H = 5.00, N = 16.27. Found C = 62.40, H = 4.58, N = 16.73; ^1H NMR (600 MHz, DMSO- d_6): δ (ppm) = 3.22 (dd, 2H, Trp CH₂, J = 9.0 Hz, 14.5 Hz), 3.24 (dd, 2H, Trp CH₂, J = 5.2 Hz, 14.5 Hz), 3.62 (s, 6H, COOCH₃), 4.69 (ddd, 2H, Trp CH, J = 7.4 Hz, 9.0 Hz, 5.2 Hz), 5.77 (s, 4H, CH₂), 6.98 (t, 2H, Trp CH, J = 7.4 Hz), 7.06 (t, 2H, Trp CH, J = 7.4 Hz), 7.19 (d, 2H, Trp CH, J = 2.2 Hz), 7.32 (d, 2H, Trp CH, J = 8.0 Hz), 7.43 (d, 4H, Ph CH, J = 8.3 Hz), 7.55 (d, 2H, Trp CH, J = 7.9 Hz), 7.84 (d, 4H, phenyl CH, J = 8.3 Hz), 7.96–8.03 (m, 3H, pyr CH), 8.70 (s, 2H, triazolyl CH), 8.81 (d, 2H, amide NH, J = 7.6 Hz), 10.81 (s, 2H, Trp NH); ^{13}C NMR (150 MHz, DMSO): δ (ppm) = 26.9 (Trp CH₂), 52.2 (CH₃), 53.0 (CH₂), 54.1 (chiral CH), 110.2 (Trp qt), 111.8 (Trp CH), 118.3 (Trp CH), 118.7 (Trp CH), 118.9 (pyr CH), 121.3 (Trp CH), 124.0 (Trp CH), 124.1 (triazolyl CH), 127.3 (Trp qt), 128.1 (Ph CH), 128.3 (Ph CH), 133.8 (Ph qt), 136.4 (Trp qt), 139.5 (Ph qt), 147.7 (triazolyl qt), 150.1 (pyr qt), 166.3 (amide C=O), 172.8 (ester C=O); FT-IR (ATR, cm⁻¹): 3441, 3388, 3158, 3057, 2954, 1738, 1639, 1611, 1576, 1525, 1496, 1459, 1437, 1347, 1280, 1217, 1197, 1176, 1152, 1089, 1046, 1021, 1012, 993, 977, 927, 864, 804, 766, 735, 674.

General Procedure for Synthesis of Ln(III) Complexes of btp Ligands. Ligand (1 or 3) (1 equiv) and Ln(CF₃SO₃)₃·6(H₂O) (0.35 equiv) were suspended in CH₃OH (6 mL) and heated to 70 °C under microwave irradiation for 20 min. The complexes were isolated as beige solids upon diffusion of diethyl ether into a CH₃OH solution.

[Eu-(1)]₃[(CF₃SO₃)₃]. HRMS (m/z) (MALDI+): Calculated for C₈₃H₆₉N₂₁O₁₈S₂F₆Eu⁺ m/z = 1978.369 [EuL₃(CF₃SO₃)₂]⁺. Found m/z = 1978.378; calculated for C₈₆H₄₆EuF₆N₁₄O₁₄S₂⁺ m/z = 1469.187 [EuL₂(CF₃SO₃)₂]⁺. Found m/z = 1469.175; calculated for C₂₉H₂₃EuF₆N₇O₁₀S₂⁺ m/z = 960.006 [EuL(CF₃SO₃)₂]⁺. Found m/z = 960.003; calculated for C₈₄H₆₉N₂₁O₂₁S₃F₉Eu·6CH₂Cl₂·1.5-(CH₃)₂NCOH, C = 50.57, H = 4.10, N = 14.04. Found C = 50.89, H = 3.60, N = 14.49. ^1H NMR (400 MHz, CD₃CN): δ = 3.91 (s, -OCH₃), 4.57 (d, 3- and 5-pyr CH), 5.52 (d, CH₂), 6.00 (d, CH₂), 6.28 (m, 4-pyr CH), 7.24 (m, Ph CH and triazolyl CH), 7.89 (d, Ph

CH); FT-IR (ATR, cm^{-1}): 3112, 2955, 1719, 1615, 1589, 1468, 1435, 1275, 1254, 1223, 1156, 1109, 1067, 1029, 963, 875, 808, 727.

[Eu-(3-Gly)₃](CF₃SO₃)₃. HRMS (*m/z*) (MALDI+): Calculated for C₉₃H₈₇N₂₇O₂₄S₂F₆Eu⁺ *m/z* = 2320.498 [EuL₃(CF₃SO₃)₂]⁺. Found *m/z* = 2320.489; calculated for C₆₄H₅₈N₁₈O₁₈S₂F₆Eu⁺ *m/z* = 1697.273 [EuL₂(CF₃SO₃)₂]⁺. Found *m/z* = 1697.282; calculated for C₉₆H₈₇N₂₇O₂₇S₃F₉Eu·1.25NaCl, C = 45.32, H = 3.45, N = 14.87. Found C = 45.67, H = 2.92, N = 14.74; ¹H NMR (400 MHz, CD₃OD): δ = 3.72 (s, 6H, OCH₃), 4.15 (m, 4H, Gly CH₂), 4.50 (d, 2H, 3- and 5-pyr CH, *J* = 7.9 Hz), 5.63 (d, 2H, CH₂, *J* = 14.3 Hz), 6.19 (d, 2H, CH₂, *J* = 14.3 Hz), 6.28 (t, 1H, 4-pyr CH, *J* = 7.8 Hz), 7.30 (d, 4H, Ph CH, *J* = 8.0 Hz), 7.47 (br s, 2H, triazolyl CH), 7.79 (d, 4H, Ph CH, *J* = 8.0 Hz); FTIR (ATR, cm^{-1}): 3345, 3101, 2956, 1737, 1643, 1617, 1572, 1541, 1504, 1467, 1454, 1438, 1248, 1222, 1160, 1122, 1067, 1029, 1011, 993, 951, 867, 847, 806, 773, 728, 659.

[Eu-(3-*l*-Ala)₃](CF₃SO₃)₃. Mp: 154–160 °C. HRMS (*m/z*) (MALDI+): Calculated for C₁₀₁H₉₉N₂₇O₂₄S₂F₆Eu⁺ *m/z* = 2404.591 [EuL₃(CF₃SO₃)₂]⁺. Found *m/z* = 2404.599; calculated for C₆₈H₆₆N₁₈O₁₈S₂F₆Eu⁺ *m/z* = 1753.336 [EuL₂(CF₃SO₃)₂]⁺. Found *m/z* = 1753.330; ¹H NMR (400 MHz, CD₃OD): δ = 1.45–1.58 (m), 3.71 (d), 3.72 (s), 4.54 (d), 4.58–4.68 (m), 5.58–5.67 (m), 6.15 (d), 6.30 (q), 7.26–7.35 (m), 7.47 (s), 7.80 (t), 8.05 (d); FTIR (ATR, cm^{-1}): 3340, 3107, 1737, 1645, 1617, 1574, 1538, 1504, 1454, 1250, 1223, 1160, 1122, 1067, 1029, 994, 807, 774, 728, 661.

[Eu-(3-*D*-Ala)₃](CF₃SO₃)₃. Mp: 151–157 °C. HRMS (*m/z*) (MALDI+): Calculated for C₁₀₁H₉₉N₂₇O₂₄F₆S₂Eu⁺ *m/z* = 2404.591 [EuL₃(CF₃SO₃)₂]⁺. Found *m/z* = 2404.571; calculated for C₆₈H₆₆N₁₈O₁₈F₆S₂Eu⁺ *m/z* = 1753.336 [EuL₂(CF₃SO₃)₂]⁺. Found *m/z* = 1753.337; ¹H NMR (400 MHz, CD₃OD): δ = 1.45–1.58 (m), 3.71 (d), 3.72 (s), 4.54 (d), 4.58–4.68 (m), 5.58–5.67 (m), 6.15 (d), 6.30 (q), 7.26–7.35 (m), 7.47 (s), 7.80 (t), 8.05 (m); FTIR (ATR, cm^{-1}): 3340, 3107, 1737, 1644, 1617, 1574, 1538, 1505, 1456, 1250, 1223, 1161, 1124, 1067, 1029, 994, 951, 807, 773, 728, 659.

[Eu-(3-*l*-Phe)₃](CF₃SO₃)₃. HRMS (*m/z*) MALDI+: Calculated for C₁₃₇H₁₂₃N₂₇O₂₄S₂F₆Eu⁺ *m/z* = 2860.7792 [EuL₃(CF₃SO₃)₂]⁺. Found *m/z* = 2860.7832; calculated for C₉₂H₈₂N₁₈O₁₈S₂F₆Eu⁺ *m/z* = 2057.461 [EuL₂(CF₃SO₃)₂]⁺. Found *m/z* = 2057.453; calculated for C₁₃₈H₁₂₃N₂₇O₂₇F₉S₃Eu·NaCl·3H₂O, C = 53.05, H = 4.16, N = 12.10. Found C = 52.62, H = 3.63, N = 11.91; ¹H NMR (400 MHz, CD₃OD): δ = 1.99 (m), 2.76 (br s), 3.06–3.19 (m), 3.45–3.47 (m), 3.69 (d), 3.73 (s), 4.45 (d), 4.86–4.97 (m), 5.51–5.60 (m), 5.96–6.13 (m), 7.01 (t), 7.10–7.18 (m), 7.19–7.31 (m), 7.42 (d), 7.63–7.72 (m), 7.77 (br s), 7.93 (d); FTIR (ATR, cm^{-1}): 3330, 3107, 1737, 1649, 1617, 1575, 1536, 1498, 1468, 1455, 1437, 1250, 1223, 1153, 1120, 1067, 1029, 994, 857, 806, 726, 700, 661.

[Eu-(3-*D*-Phe)₃](CF₃SO₃)₃. HRMS (*m/z*) MALDI+: Calculated for C₁₃₇H₁₂₃N₂₇O₂₄S₂F₆Eu⁺ *m/z* = 2860.779 [EuL₃(CF₃SO₃)₂]⁺. Found *m/z* = 2860.787; calculated for C₉₂H₈₂N₁₈O₁₈S₂F₆Eu⁺ *m/z* = 2057.461 [EuL₂(CF₃SO₃)₂]⁺. Found *m/z* = 2057.458; calculated for C₁₃₈H₁₂₃N₂₇O₂₇F₉S₃Eu·1.25NaCl·3H₂O, C = 52.81, H = 4.14, N = 12.05. Found C = 53.22, H = 3.65, N = 11.92; ¹H NMR (400 MHz, CD₃OD): δ = 1.99 (m), 2.76 (br s), 3.06–3.19 (m), 3.45–3.47 (m), 3.69 (d), 3.73 (s), 4.45 (d), 4.86–4.97 (m), 5.51–5.60 (m), 5.96–6.13 (m), 7.01 (m), 7.10–7.18 (m), 7.19–7.31 (m), 7.42 (d), 7.63–7.72 (m), 7.77 (br s), 7.93 (d); FTIR (ATR, cm^{-1}): 3330, 3107, 1735, 1648, 1617, 1575, 1536, 1498, 1468, 1455, 1437, 1251, 1223, 1153, 1120, 1067, 1029, 993, 857, 806, 726, 701, 661.

[Eu-(3-*l*-Trp)₃](CF₃SO₃)₃. Mp: 164–171 °C. HRMS (*m/z*) (MALDI+): Calculated for C₁₄₉H₁₂₉N₃₃O₂₄F₆S₂Eu⁺ *m/z* = 3094.845 [EuL₃(CF₃SO₃)₂]⁺. Found *m/z* = 3094.852; calculated for C₁₀₀H₈₆N₂₂O₁₈F₆S₂Eu⁺ *m/z* = 2212.497 [EuL₂(CF₃SO₃)₂]⁺. Found *m/z* = 2212.507; ¹H NMR (400 MHz, CD₃OD): δ = 0.88 (m), 1.15 (t), 1.27 (m), 2.13 (s), 2.76 (br s), 3.11 (s), 3.28 (m), 3.46 (s), 3.66 (m), 4.31 (d), 4.55 (s), 4.82 (br s), 5.47 (d), 5.70 (s), 5.94 (d), 6.37 (s), 6.93 (t), 7.03 (m), 7.11 (m), 7.18 (m), 7.26 (d), 7.38 (d), 7.50 (d), 7.59 (m), 7.71 (d), 7.93 (br s), 8.54 (br s); FTIR (ATR, cm^{-1}): 3313, 3101, 2953, 1736, 1648, 1618, 1573, 1535, 1500, 1458, 1435, 1341, 1249, 1223, 1156, 1121, 1097, 1067, 1029, 1010, 994, 806, 742, 660.

[Eu-(3-*D*-Trp)₃](CF₃SO₃)₃. Mp: 168–173 °C. HRMS (*m/z*) (MALDI+): Calculated for C₁₄₉H₁₂₉N₃₃O₂₄F₆S₂Eu⁺ *m/z* = 3094.845 [EuL₃(CF₃SO₃)₂]⁺. Found *m/z* = 3094.860; calculated for C₁₀₀H₈₆N₂₂O₁₈F₆S₂Eu⁺ *m/z* = 2212.497 [EuL₂(CF₃SO₃)₂]⁺. Found *m/z* = 2212.502; ¹H NMR (400 MHz, CD₃OD): δ = 0.90 (m), 1.16 (t), 1.27 (m), 2.13 (s), 2.78 (br s), 3.11 (s), 3.29 (m), 3.46 (s), 3.67 (m), 4.31 (d), 4.55 (s), 4.83 (br s), 5.47 (d), 5.71 (s), 5.94 (d), 6.37 (s), 6.95 (t), 7.03 (m), 7.12 (m), 7.20 (m), 7.27 (d), 7.40 (d), 7.52 (d), 7.61 (m), 7.72 (d), 7.94 (br s), 8.55 (br s); FTIR (ATR, cm^{-1}): 3312, 3110, 2953, 1735, 1642, 1618, 1573, 1534, 1500, 1458, 1437, 1341, 1249, 1222, 1156, 1123, 1097, 1066, 1029, 1010, 993, 806, 741, 660.

[Tb-(1)₃](CF₃SO₃)₃. HRMS (*m/z*) MALDI+: Calculated for C₈₃H₆₉N₂₁O₁₈S₂F₆Tb⁺ *m/z* = 1984.373 [TbL₃(CF₃SO₃)₂]⁺. Found *m/z* = 1984.370; calculated for C₅₆H₄₆N₁₄O₁₄S₂F₆Tb⁺ *m/z* = 1475.192 [TbL₂(CF₃SO₃)₂]⁺. Found *m/z* = 1475.191; calculated for C₈₄H₆₉N₂₁O₂₁S₃F₉Tb·2.5NaCl·4CH₃OH, C = 43.88, H = 3.56, N = 12.21. Found C = 44.10, H = 3.26, N = 11.67; ¹H NMR (400 MHz, CD₃CN): δ = -0.41 (br s), 1.77 (s), 2.68 (br s), 2.78 (s), 2.90 (s), 3.25 (br s), 3.89 (s), 5.02 (br s), 5.71 (s), 6.16 (br s), 6.63 (br s), 7.28 (s), 7.43 (d), 7.59 (s), 8.01 (d), 8.37 (s), 9.61 (br s); FTIR (ATR, cm^{-1}): 3119, 2956, 1716, 1616, 1589, 1435, 1253, 1223, 1154, 1108, 1068, 1028, 807, 727, 661.

[Tb-(3-Gly)₃](CF₃SO₃)₃. HRMS (*m/z*) MALDI+: Calculated for C₉₅H₈₇N₂₇O₂₄S₂F₆Tb⁺ *m/z* = 2326.502 [TbL₃(CF₃SO₃)₂]⁺. Found *m/z* = 2326.509; calculated for C₆₄H₅₈N₁₈O₁₈S₂F₆Tb⁺ *m/z* = 1703.278 [TbL₂(CF₃SO₃)₂]⁺. Found *m/z* = 1703.273; calculated for C₉₆H₈₇N₂₇O₂₇S₃F₉Tb·NaCl, C = 45.48, H = 3.46, N = 14.92. Found C = 45.67, H = 2.92, N = 14.74; ¹H NMR (400 MHz, CD₃CN): δ = 1.39 (br s), 1.77 (m), 2.57 (br s), 3.70 (br s), 3.88 (br s), 4.22 (br m), 4.90 (br s), 5.45 (s), 5.69 (s), 6.49 (br s), 7.12 (br s), 7.91 (br m), 10.77 (br s); FTIR (ATR, cm^{-1}): 3345, 3106, 2953, 1741, 1649, 1618, 1589, 1574, 1541, 1505, 1469, 1455, 1438, 1408, 1370, 1247, 1213, 1183, 1158, 1123, 1068, 1060, 1029, 1011, 995, 976, 867, 849, 807, 773, 757, 729, 709, 691, 660.

[Tb-(3-*l*-Ala)₃](CF₃SO₃)₃. HRMS (*m/z*) MALDI+: Calculated for C₁₀₁H₉₉N₂₇O₂₄S₂F₆Tb⁺ *m/z* = 2410.596 [TbL₃(CF₃SO₃)₂]⁺. Found *m/z* = 2410.602; calculated for C₁₀₂H₉₉N₂₇O₂₇S₃F₉Tb·3.1-(CH₃)₂NCOH, C = 47.95, H = 4.36, N = 15.12. Found C = 48.50, H = 3.83, N = 14.90; ¹H NMR (400 MHz, CD₃OD): δ = -2.48, 1.77, 2.65 (br s), 3.70 (s), 3.79 (s), 4.32–4.52 (m), 5.45 (s), 5.69 (s), 6.65–6.75 (br m), 7.18 (br s), 7.29 (br s), 7.42 (d), 7.59 (s), 7.83 (d), 8.02 (d), 8.36 (s), 10.30 (br s); FTIR (ATR, cm^{-1}): 3348, 3170, 2957, 1741, 1642, 1617, 1577, 1531, 1504, 1458, 1438, 1425, 1379, 1358, 1346, 1271, 1238, 1213, 1163, 1095, 1080, 1068, 1045, 1029, 1021, 993, 980, 938, 876, 849, 841, 801, 790, 775, 759, 742, 730, 660.

[Tb-(3-*D*-Ala)₃](CF₃SO₃)₃. HRMS (*m/z*) MALDI+: Calculated for C₁₀₁H₉₉N₂₇O₂₄S₂F₆Tb⁺ *m/z* = 2410.596 [TbL₃(CF₃SO₃)₂]⁺. Found *m/z* = 2410.602; ¹H NMR (400 MHz, CD₃OD): δ = -2.48, 1.77, 2.65 (br s), 3.67 (m), 3.77 (s), 4.10–4.50 (m), 5.45 (s), 5.69 (s), 6.06 (br s), 6.58 (br s), 7.05 (br s), 7.18 (br s), 7.29 (br s), 7.42 (d), 7.59 (s), 7.83 (d), 8.02 (d), 8.36 (s), 10.15 (br s); FTIR (ATR, cm^{-1}): 3350, 3167, 2957, 1741, 1642, 1617, 1577, 1534, 1504, 1457, 1438, 1426, 1379, 1358, 1346, 1271, 1239, 1214, 1163, 1095, 1080, 1068, 1045, 1029, 1021, 993, 980, 938, 876, 849, 841, 802, 790, 775, 759, 742, 730, 660.

[Tb-(3-*l*-Phe)₃](CF₃SO₃)₃. HRMS (*m/z*) MALDI+: Calculated for C₁₃₇H₁₂₃N₂₇O₂₄S₂F₆Tb⁺ *m/z* = 2866.783 [TbL₃(CF₃SO₃)₂]⁺. Found *m/z* = 2866.784; calculated for C₁₃₈H₁₂₃N₂₇O₂₇F₉S₃Tb·1.25NaCl·0.5H₂O, C = 53.47, H = 4.03, N = 12.20. Found C = 53.25, H = 3.50, N = 12.01; ¹H NMR (400 MHz, CD₃CN): δ = 1.00 (s), 1.25 (m), 1.77 (s), 2.58 (br m), 2.82 (m), 3.00–3.22 (m), 3.52 (s), 3.68 (s), 3.72 (s), 4.59 (br s), 4.71 (br s), 5.68 (s), 6.11 (br s), 6.57 (br s), 6.75 (br s), 7.08–7.25 (m), 7.73 (m), 8.35 (s), 9.60 (br s); FTIR (ATR, cm^{-1}): 3312, 2955, 1737, 1645, 1617, 1573, 1536, 1498, 1469, 1455, 1436, 1250, 1222, 1154, 1121, 1097, 1067, 1029, 994, 875, 806, 727, 700, 660.

[Tb-(3-*D*-Phe)₃](CF₃SO₃)₃. HRMS (*m/z*) MALDI+: Calculated for C₁₃₇H₁₂₃N₂₇O₂₄S₂F₆Tb⁺ *m/z* = 2866.783 [TbL₃(CF₃SO₃)₂]⁺. Found *m/z* = 2866.773; calculated for C₉₂H₈₂N₁₈O₁₈F₆S₂Tb⁺ *m/z* = 2063.465

[EuL₂(CF₃SO₃)₂]⁺. Found *m/z* = 2063.465; calculated for C₁₃₈H₁₂₃N₂₇O₂₇F₉S₃Tb·NaCl·2.5H₂O, C = 53.01, H = 4.13, N = 12.12. Found C = 52.62, H = 3.63, N = 11.91; ¹H NMR (400 MHz, CD₃CN): δ = 1.00 (s), 1.25 (m), 1.77 (quin), 2.25 (br m), 2.70 (br m), 2.85 (m), 3.00–3.28 (m), 3.51 (s), 3.68 (s), 3.73 (s), 4.58 (br s), 4.71 (br s), 5.68 (s), 6.10 (br s), 6.59 (br s), 6.72 (br s), 7.08–7.25 (m), 7.72 (m), 8.35 (s), 9.70 (s); FTIR (ATR, cm⁻¹): 3313, 2981, 1736, 1643, 1617, 1573, 1535, 1498, 1469, 1456, 1437, 1249, 1222, 1153, 1121, 1096, 1067, 1029, 994, 859, 806, 727, 700, 660.

[Tb·(3-*l*-Trp)₃](CF₃SO₃)₃. HRMS (*m/z*) MALDI+: Calculated for C₁₄₉H₁₂₉N₃₃O₂₄F₆S₂Tb⁺ *m/z* = 3100.849 [TbL₃(CF₃SO₃)₂]⁺. Found *m/z* = 3100.842; calculated for C₁₅₀H₁₂₉N₃₃O₂₇F₉S₃Tb·NaCl·6H₂O, C = 52.70, H = 4.16, N = 13.52. Found C = 52.91, H = 3.61, N = 13.44; ¹H NMR (400 MHz, CD₃CN): δ = 9.48 (br d), 8.33 (br s), 8.01 (m), 7.73 (d), 7.57 (m), 7.47 (m), 7.37 (d), 7.21 (m), 7.14 (m), 7.02 (m), 6.80 (s), 6.48 (br s), 5.67 (br s), 5.45 (s), 4.89 (m), 4.07 (q), 3.76 (br s), 3.66 (br s), 3.61 (br s), 3.28 (m), 1.77 (q), 1.19 (t), 1.00 (s), -2.48 (s); FTIR (ATR, cm⁻¹): 3311, 2981, 1736, 1648, 1618, 1573, 1534, 1500, 1458, 1437, 1342, 1250, 1223, 1157, 1124, 1097, 1067, 1029, 994, 807, 743, 659.

[Tb·(3-*D*-Trp)₃](CF₃SO₃)₃. HRMS (*m/z*) MALDI+: Calculated for C₁₄₉H₁₂₉N₃₃O₂₄F₆S₂Tb⁺ *m/z* = 3100.849 [TbL₃(CF₃SO₃)₂]⁺. Found *m/z* = 3100.862; calculated for C₁₅₀H₁₂₉N₃₃O₂₇F₉S₃Tb·0.75H₂O, C = 55.17, H = 4.03, N = 14.15. Found C = 54.68, H = 3.83, N = 13.98; ¹H NMR (400 MHz, CD₃CN): δ = 9.66 (br s), 9.19 (s), 8.33 (br s), 8.01 (m), 7.73 (d), 7.56 (m), 7.37 (d), 7.26 (m), 7.19 (m), 7.12 (m), 7.02 (m), 6.79 (s), 6.66 (br s), 5.67 (br s), 5.45 (s), 4.90 (m), 4.07 (q), 3.82 (br s), 3.67 (d), 3.56 (m), 3.28 (d), 1.77 (q), 1.21 (t), 1.00 (s), -2.48 (s); FTIR (ATR, cm⁻¹): 3327, 2981, 1734, 1645, 1618, 1574, 1532, 1501, 1458, 1436, 1343, 1250, 1223, 1157, 1124, 1097, 1067, 1029, 994, 806, 742, 660.

■ ASSOCIATED CONTENT

● Supporting Information

¹H NMR, ¹³C NMR, and 2D NMR spectra of ligands; ¹H NMR spectra of complexes; selective ROESY and TOCSY spectra of **1** and [Eu(1)₃](CF₃SO₃)₃; IR spectra; HRMS isotopic pattern matching; UV–vis absorption, luminescence and excitation spectra of ligands and complexes; CPL spectra of [Tb·(3-*l*-Trp)₃](CF₃SO₃)₃; further discussion of spectroscopic titrations; and full titration data, calculated binding isotherms and speciation diagrams. This material is available free of charge via the Internet at <http://pubs.acs.org>.

■ AUTHOR INFORMATION

Corresponding Author

*E-mail: gunnlaut@tcd.ie. Fax: +353 1 716 2628. Tel: +353 1 896 3459.

Notes

The authors declare no competing financial interest.

■ ACKNOWLEDGMENTS

We thank the Irish Research Council (Embark Initiative) and TCD School of Chemistry for studentships funding this work (J.P.B.), IRCSET for postdoctoral fellowship (J.A.K.) and Science Foundation Ireland (SFI) for SFI PI 2010 (10/IN.1/B2999) and SFI PI 2013 (13/IA/1865) funding. We thank Dr. Martin Feeney for HRMS measurements, Dr. Manuel Ruether for technical assistance, and Dr. Oxana Kotova and Dr. Salvador Blasco for useful discussions.

■ REFERENCES

- (1) Li, Y.; Huffman, J. C.; Flood, A. H. *Chem. Commun.* **2007**, 2692–2694.
- (2) Crowley, J. D.; Bandeen, P. H.; Hanton, L. R. *Polyhedron* **2010**, 29, 70–83.

- (3) Crowley, J. D.; Bandeen, P. H. *Dalton Trans.* **2010**, 39, 612–623.
- (4) Li, Y.; Flood, A. H. *Angew. Chem., Int. Ed.* **2008**, 47, 2649–2652.
- (5) Li, Y.; Flood, A. H. *J. Am. Chem. Soc.* **2008**, 130, 12111–12122.
- (6) Zahran, E. M.; Hua, Y.; Lee, S.; Flood, A. H.; Bachas, L. G. *Anal. Chem.* **2011**, 83, 3455–3461.
- (7) Meudtner, R. M.; Hecht, S. *Macromol. Rapid Commun.* **2008**, 29, 347–351.
- (8) Berlin, M.-A.; Ostermeier, M.; Meudtner, R. M.; Limberg, C.; Hecht, S. *Polym. Prepr.* **2009**, 50, 261.
- (9) Zornik, D.; Meudtner, R. M.; El Malah, T.; Thiele, C. M.; Hecht, S. *Chem.—Eur. J.* **2011**, 17, 1473–1484.
- (10) Meudtner, R. M.; Ostermeier, M.; Goddard, R.; Limberg, C.; Hecht, S. *Chem.—Eur. J.* **2007**, 13, 9834–9840.
- (11) Schulze, B.; Friebe, C.; Hager, M. D.; Winter, A.; Hoogenboom, R.; Görls, H.; Schubert, U. S. *Dalton Trans.* **2009**, 787–794.
- (12) Schulze, B.; Friebe, C.; Hager, M. D.; Winter, A.; Hoogenboom, R.; Görls, H.; Schubert, U. S. *Polym. Prepr.* **2009**, 50, 252.
- (13) Schulze, B.; Friebe, C.; Hager, M. D.; Winter, A.; Schubert, U. S. *Polym. Prepr.* **2009**, 50, 576.
- (14) Schulze, B.; Friebe, C.; Hoepfner, S.; Pavlov, G. M.; Hager, M. D.; Winter, A.; Schubert, U. S. *Polym. Prepr.* **2011**, 52, 917–918.
- (15) Schulze, B.; Friebe, C.; Hoepfner, S.; Pavlov, G. M.; Winter, A.; Hager, M. D.; Schubert, U. S. *Macromol. Rapid Commun.* **2012**, 33, 597–602.
- (16) Zhang, C.; Shen, X.; Sakai, R.; Gottschaldt, M.; Schubert, U. S.; Hirohara, S.; Tanihara, M.; Yano, S.; Obata, M.; Xiao, N.; Satoh, T.; Kakuchi, T. *J. Polym. Sci., Part A: Polym. Chem.* **2011**, 49, 746–753.
- (17) Byrne, J. P.; Kitchen, J. A.; Gunnlaugsson, T. *Chem. Soc. Rev.* **2014**, 43, 5302–5325.
- (18) Munuera, L.; O'Reilly, R. K. *Dalton Trans.* **2010**, 39, 388–391.
- (19) Brunet, E.; Juanes, O.; Jiménez, L.; Rodríguez-Ubis, J. C. *Tetrahedron Lett.* **2009**, 50, 5361–5363.
- (20) Byrne, J. P.; Kitchen, J. A.; Kotova, O.; Leigh, V.; Bell, A.; Boland, J. J.; Albrecht, M.; Gunnlaugsson, T. *Dalton Trans.* **2014**, 43, 196–209.
- (21) Chan, T. R.; Hilgraf, R.; Sharpless, K. B.; Fokin, V. V. *Org. Lett.* **2004**, 6, 2853–2855.
- (22) Danielraj, P.; Varghese, B.; Sankararaman, S. *Acta Crystallogr., Sect. C* **2010**, 66, m366–m370.
- (23) Ostermeier, M.; Berlin, M.-A.; Meudtner, R. M.; Demeshko, S.; Meyer, F.; Limberg, C.; Hecht, S. *Chem.—Eur. J.* **2010**, 16, 10202–10213.
- (24) Li, Y.; Zhao, L.; Tam, A. Y.-Y.; Wong, K. M.-C.; Wu, L.; Yam, V. W.-W. *Chem.—Eur. J.* **2013**, 19, 14496–14505.
- (25) Lang, C.; Pahnke, K.; Kiefer, C.; Goldmann, A. S.; Roesky, P. W.; Barner-Kowollik, C. *Polym. Chem.* **2013**, 4, 5456–5462.
- (26) Younes, A. H.; Clark, R. J.; Zhu, L. *Supramol. Chem.* **2012**, 24, 696–706.
- (27) Schulze, B.; Escudero, D.; Friebe, C.; Siebert, R.; Görls, H.; Köhn, U.; Altuntas, E.; Baumgaertel, A.; Hager, M. D.; Winter, A.; Dietzek, B.; Popp, J.; González, L.; Schubert, U. S. *Chem.—Eur. J.* **2011**, 17, 5494–5498.
- (28) Schulze, B.; Escudero, D.; Friebe, C.; Siebert, R.; Görls, H.; Sinn, S.; Thomas, M.; Mai, S.; Popp, J.; Dietzek, B.; González, L.; Schubert, U. S. *Chem.—Eur. J.* **2012**, 18, 4010–4025.
- (29) Fletcher, J. T.; Bumgarner, B. J.; Engels, N. D.; Skoglund, D. A. *Organomet.* **2008**, 27, 5430–5433.
- (30) Floquet, S.; Borkovec, M.; Bernardinelli, G.; Pinto, A.; Leuthold, L.-A.; Hopfgartner, G.; Imbert, D.; Bünzli, J.-C. G.; Piguet, C. *Chem.—Eur. J.* **2004**, 10, 1091–1105.
- (31) Eliseeva, S. V.; Bünzli, J.-C. G. *Chem. Soc. Rev.* **2010**, 39, 189–227.
- (32) Bünzli, J.-C. G.; Piguet, C. *Chem. Soc. Rev.* **2005**, 34, 1048–1077.
- (33) Kido, J.; Okamoto, Y. *Chem. Rev.* **2002**, 102, 2357–2368.
- (34) Leonard, J. P.; Jensen, P.; McCabe, T.; O'Brien, J. E.; Peacock, R. D.; Kruger, P. E.; Gunnlaugsson, T. *J. Am. Chem. Soc.* **2007**, 129, 10986–10987.

- (35) Lincheneau, C.; Peacock, R. D.; Gunnlaugsson, T. *Chem.—Asian J.* **2010**, *5*, 500–504.
- (36) Lincheneau, C.; Destribats, C.; Barry, D. E.; Kitchen, J. A.; Peacock, R. D.; Gunnlaugsson, T. *Dalton Trans.* **2011**, *40*, 12056–12059.
- (37) Lincheneau, C.; Jean-Denis, B.; Gunnlaugsson, T. *Chem. Commun.* **2014**, *50*, 2857–2860.
- (38) Barry, D. E.; Kitchen, J. A.; Albrecht, M.; Faulkner, S.; Gunnlaugsson, T. *Langmuir* **2013**, *29*, 11506–11515.
- (39) Kitchen, J. A.; Barry, D. E.; Mercks, L.; Albrecht, M.; Peacock, R. D.; Gunnlaugsson, T. *Angew. Chem., Int. Ed.* **2012**, *51*, 704–708.
- (40) Kotova, O.; Daly, R.; dos Santos, C. M. G.; Boese, M.; Kruger, P. E.; Boland, J. J.; Gunnlaugsson, T. *Angew. Chem., Int. Ed.* **2012**, *51*, 7208–7212.
- (41) Martin, N.; Bünzli, J.-C. G.; McKee, V.; Piguët, C.; Hopfgartner, G. *Inorg. Chem.* **1998**, *37*, 577–589.
- (42) Escande, A.; Guénée, L.; Buchwalder, K.-L.; Piguët, C. *Inorg. Chem.* **2009**, *48*, 1132–1147.
- (43) Shavaleev, N. M.; Eliseeva, S. V.; Scopelliti, R.; Bünzli, J.-C. G. *Inorg. Chem.* **2010**, *49*, 3927–3936.
- (44) de Bettencourt-Dias, A.; Barber, P. S.; Bauer, S. J. *Am. Chem. Soc.* **2012**, *134*, 6987–6994.
- (45) de Bettencourt-Dias, A.; Barber, P. S.; Viswanathan, S.; de Lill, D. T.; Rollett, A.; Ling, G.; Altun, S. *Inorg. Chem.* **2010**, *49*, 8848–8861.
- (46) de Bettencourt-Dias, A.; Viswanathan, S.; Rollett, A. *J. Am. Chem. Soc.* **2007**, *129*, 15436–15437.
- (47) Andreiadis, E. S.; Imbert, D.; Pecaut, J.; Demadrille, R.; Mazzanti, M. *Dalton Trans.* **2012**, *41*, 1268–1277.
- (48) Di Pietro, S.; Imbert, D.; Mazzanti, M. *Chem. Commun.* **2014**, *50*, 10323–10326.
- (49) Chandrasekhar, N.; Chandrasekar, R. *J. Org. Chem.* **2010**, *75*, 4852–4855.
- (50) Brunet, E.; Jiménez, L.; de Victoria-Rodriguez, M.; Luu, V.; Muller, G.; Juanes, O.; Rodríguez-Ubis, J. C. *Microporous Mesoporous Mater.* **2013**, *169*, 222–234.
- (51) Indapurkar, A.; Henriksen, B.; Tolman, J.; Fletcher, J. *J. Pharm. Sci.* **2013**, *102*, 2589–2598.
- (52) Bonnet, C. S.; Devocelle, M.; Gunnlaugsson, T. *Org. Biomol. Chem.* **2012**, *10*, 126–133.
- (53) Nitz, M.; Franz, K. J.; Maglathlin, R. L.; Imperiali, B. *ChemBioChem.* **2003**, *4*, 272–276.
- (54) MacManus, J. P.; Hogue, C. W.; Marsden, B. J.; Sikorska, M.; Szabo, A. G. *J. Biol. Chem.* **1990**, *265*, 10358–10366.
- (55) Lincheneau, C.; Leonard, J. P.; McCabe, T.; Gunnlaugsson, T. *Chem. Commun.* **2011**, *47*, 7119–7121.
- (56) Kotova, O.; Kitchen, J. A.; Lincheneau, C.; Peacock, R. D.; Gunnlaugsson, T. *Chem.—Eur. J.* **2013**, *19*, 16181–16186.
- (57) Molloy, J. K.; Kotova, O.; Peacock, R. D.; Gunnlaugsson, T. *Org. Biomol. Chem.* **2012**, *10*, 314–322.
- (58) Stomeo, F.; Lincheneau, C.; Leonard, J. P.; O'Brien, J. E.; Peacock, R. D.; McCoy, C. P.; Gunnlaugsson, T. *J. Am. Chem. Soc.* **2009**, *131*, 9636–9637.
- (59) Hua, K. T.; Xu, J.; Quiroz, E. E.; Lopez, S.; Ingram, A. J.; Johnson, V. A.; Tisch, A. R.; de Bettencourt-Dias, A.; Straus, D. A.; Muller, G. *Inorg. Chem.* **2011**, *51*, 647–660.
- (60) Carr, R.; Evans, N. H.; Parker, D. *Chem. Soc. Rev.* **2012**, *41*, 7673–7686.
- (61) Matsumoto, K.; Suzuki, K.; Tsukuda, T.; Tsubomura, T. *Inorg. Chem.* **2010**, *49*, 4717–4719.
- (62) Muller, G.; Maupin, C. L.; Riehl, J. P.; Birkedal, H.; Piguët, C.; Bünzli, J.-C. G. *Eur. J. Inorg. Chem.* **2003**, *2003*, 4065–4072.
- (63) Dickins, R. S.; Howard, J. A. K.; Maupin, C. L.; Moloney, J. M.; Parker, D.; Riehl, J. P.; Siligardi, G.; Williams, J. A. G. *Chem.—Eur. J.* **1999**, *5*, 1095–1105.
- (64) Dickins, R. S.; Howard, J. A. K.; Maupin, C. L.; Moloney, J. M.; Parker, D.; Peacock, R. D.; Riehl, J. P.; Siligardi, G. *New J. Chem.* **1998**, *22*, 891–899.
- (65) Smith, D. G.; McMahon, B. K.; Pal, R.; Parker, D. *Chem. Commun.* **2012**, *48*, 8520–8522.
- (66) Muller, G. *Dalton Trans.* **2009**, 9692–9707.
- (67) Parker, D. *Coord. Chem. Rev.* **2000**, *205*, 109–130.
- (68) Bonnet, C. S.; Gunnlaugsson, T. *New J. Chem.* **2009**, *33*, 1025–1030.
- (69) Horrocks, W. D.; Sudnick, D. R. *Acc. Chem. Res.* **1981**, *14*, 384–392.
- (70) Beeby, A.; Clarkson, I. M.; Dickins, R. S.; Faulkner, S.; Parker, D.; Royle, L.; de Sousa, A. S.; Williams, J. A. G.; Woods, M. *J. Chem. Soc., Perkin Trans. 2* **1999**, 493–504.
- (71) Chauvin, A. S.; Gumy, F.; Imbert, D.; Bünzli, J. C. G. *Spectrosc. Lett.* **2004**, *37*, 517–532.
- (72) Chauvin, A.-S.; Gumy, F.; Imbert, D.; Bünzli, J.-C. G. *Spectrosc. Lett.* **2007**, *40*, 193–193.
- (73) Crosby, G. A.; Demas, J. N. *J. Phys. Chem.* **1971**, *75*, 991–1024.
- (74) Le Borgne, T.; Benech, J.-M.; Floquet, S.; Bernardinelli, G.; Aliprandini, C.; Bettens, P.; Piguët, C. *Dalton Trans.* **2003**, 3856–3868.
- (75) Neil, E. R.; Funk, A. M.; Yufit, D. S.; Parker, D. *Dalton Trans.* **2014**, *43*, 5490–5504.
- (76) Walton, J. W.; Carr, R.; Evans, N. H.; Funk, A. M.; Kenwright, A. M.; Parker, D.; Yufit, D. S.; Botta, M.; De Pinto, S.; Wong, K.-L. *Inorg. Chem.* **2012**, *51*, 8042–8056.
- (77) Ouali, N.; Bocquet, B.; Rigault, S.; Morgantini, P.-Y.; Weber, J.; Piguët, C. *Inorg. Chem.* **2002**, *41*, 1436–1445.
- (78) Chandrasekhar, N.; Chandrasekar, R. *Angew. Chem., Int. Ed.* **2012**, *51*, 3556–3561.
- (79) *ReactLab Equilibria*; Jplus Consulting Pty Ltd; <http://jplusconsulting.com/products/reactlab-equilibria/> (5 November 2014).
- (80) Muller, G.; Schmidt, B.; Jiricek, J.; Hopfgartner, G.; Riehl, J. P.; Bünzli, J.-C. G.; Piguët, C. *J. Chem. Soc., Dalton Trans.* **2001**, 2655–2662.